




ORIGINAL RESEARCH

# Macrophage Polarization in the Perivascular Fat Was Associated With Coronary Atherosclerosis

Daniela Souza Farias-Itao , BSN, MSc; Carlos Augusto Pasqualucci, MD, PhD; Renato Araújo de Andrade, BE, PSM; Luiz Fernando Ferraz da Silva, MD, PhD; Maristella Yahagi-Estevam, BPT; Sílvia Helena Gelas Lage , MD, PhD; Renata Elaine Paraízo Leite, BPT, PhD; Alexandre Brincalpe Campo, BE, PhD; Claudia Kimie Suemoto , MD, MSc, PhD

**BACKGROUND:** Inflammation of the perivascular adipose tissue (PvAT) may be related to atherosclerosis; however, the association of polarized macrophages in the pericoronary PvAT with measurements of atherosclerosis components in humans has not been fully investigated.

**METHODS AND RESULTS:** Coronary arteries were dissected with surrounding PvAT. We evaluated the percentage of arterial obstruction, intima-media thickness, fibrous cap thickness, plaque components, and the number of vasa vasorum. The number of proinflammatory (M1) and anti-inflammatory (M2) macrophages in the periplate and control PvAT were evaluated using immunohistochemistry. Regression models adjusted for sociodemographic and clinical variables were used. In 319 segments from 82 individuals, we found a correlation of the M1/M2 macrophage density ratio with an increase in arterial obstruction ( $P=0.02$ ) and lipid content ( $P=0.01$ ), and a decrease in smooth muscle cells ( $P=0.02$ ). M1 and the ratio of M1/M2 macrophages were associated with an increased risk of thrombosis ( $P=0.03$ ). In plaques with thrombosis, M1 macrophages were correlated with a decrease in fibrous cap thickness ( $P=0.006$ ), an increase in lipid content ( $P=0.008$ ), and the number of vasa vasorum in the adventitia layer ( $P=0.001$ ). M2 macrophages were correlated with increased arterial obstruction ( $P=0.01$ ), calcification ( $P=0.02$ ), necrosis ( $P=0.03$ ) only in plaques without thrombosis, and decrease of the number of vasa vasorum in plaques with thrombosis ( $P=0.003$ ).

**CONCLUSIONS:** M1 macrophages in the periplate PvAT were associated with a higher risk of coronary thrombosis and were correlated with histological components of plaque progression and destabilization. M2 macrophages were correlated with plaque size, calcification, necrotic content, and a decrease in the number of vasa vasorum in the adventitia layer.

**Key Words:** atherosclerosis ■ coronary artery disease ■ inflammation ■ macrophages ■ pericoronary adipose tissue

Atherosclerosis is the main cause of cardiovascular diseases, accounting for 85% of cardiovascular disease deaths.<sup>1</sup> Among them, coronary heart disease is the main disease (42%) and has increased in recent years despite a decline from 1980 to 2010.<sup>2</sup> Atherosclerosis has complex pathophysiology, with an intense biochemical activity that is modulated by several risk factors. Among them, inflammation plays

a central role.<sup>3</sup> In the last decade, inflammation in the perivascular adipose tissue (PvAT) has been linked to development and severity of coronary atherosclerosis. PvAT comes into direct contact with the adventitia layer and other characteristics, making it the ideal environment for the recruitment of immune cells.<sup>4</sup>

In animal models, inflammation in the PvAT was related to the percentage of arterial obstruction,

Correspondence to: Daniela Souza Farias-Itao, BSN, MSc, Faculdade de Medicina da Universidade de São Paulo, 455 Avenida Doutor Arnaldo, Sala 1355, 01246-903, São Paulo, Brazil. E-mail: dsfarias@usp.br

Supplemental Material is available at <https://www.ahajournals.org/doi/suppl/10.1161/JAHA.121.023274>

For Sources of Funding and Disclosures, see page 11.

© 2022 The Authors. Published on behalf of the American Heart Association, Inc., by Wiley. This is an open access article under the terms of the Creative Commons Attribution-NonCommercial-NoDerivs License, which permits use and distribution in any medium, provided the original work is properly cited, the use is non-commercial and no modifications or adaptations are made.

JAHA is available at: [www.ahajournals.org/journal/jaha](http://www.ahajournals.org/journal/jaha)

## CLINICAL PERSPECTIVE

### What Is New?

- Proinflammatory macrophages in the perivascular adipose tissue were associated with higher thrombosis risk and plaque destabilization.
- Proinflammatory phenotype was correlated with the decrease of fibrous cap thickness and directly correlated with the increase of lipid area and the number of vasa vasorum in the adventitia layer.
- In plaques without thrombosis, anti-inflammatory macrophages were associated with arterial obstruction, calcification, and necrotic content.

### What Are the Clinical Implications?

- This translational study suggests mechanisms of how polarized macrophages in the perivascular adipose tissue are related to coronary atherosclerosis and plaque.
- Currently, clinical trials are testing whether immunological agents could prevent or block atherosclerotic plaque development.
- Immunological agents that act in the inflammatory pathway between proinflammatory macrophages in the perivascular adipose tissue and coronary atherosclerosis may be promising therapeutic options.

## Nonstandard Abbreviations and Acronyms

<b>APA</b>	atherosclerotic plaque analyzer
<b>FCT</b>	fibrous cap thickness
<b>IMT</b>	intima-media thickness
<b>NOK</b>	next of kin
<b>PvAT</b>	perivascular adipose tissue
<b>SMC</b>	smooth muscle cell

intima-media thickness (IMT), lipid-rich plaque, and the presence of atherothrombosis. Moreover, macrophage infiltration in the PvAT preceded atherosclerotic plaque formation in other animal studies.<sup>5,6</sup> In humans, macrophage infiltration in the coronary PvAT was associated with CAD (coronary artery disease).<sup>7-13</sup> The inflammation mediated by polarized macrophages in the coronary PvAT was higher in patients with CAD in comparison with other areas (eg, aorta, internal thoracic artery, and saphenous vein).<sup>12,14</sup> However, these studies did not evaluate plaque composition or plaque instability.<sup>7-11</sup> We previously demonstrated that macrophages in the periplaque PvAT in coronary arteries

were associated with the percentage of arterial obstruction and with the presence of unstable plaques. These associations were greater in periplaque PvAT than in control PvAT, but the phenotype predominance remains unclear.<sup>13</sup> Proinflammatory macrophages (M1) in the PvAT were more frequent among patients with CAD,<sup>7,8</sup> but another study found no association.<sup>11</sup> The association of anti-inflammatory macrophages (M2) with CAD also showed mixed results.<sup>8-11</sup> The ratio of M1 to M2 macrophages, a marker of the proinflammatory state, was higher in patients with CAD and was correlated with atherosclerosis severity.<sup>9,10</sup> However, it remains unknown whether macrophage polarization in the PvAT is correlated with plaque components and size in humans.

Therefore, we investigated the association of macrophage polarization in the surrounding PvAT with the atherosclerotic plaque components and morphometric measurements in human coronary arteries from individuals who submitted to a full-body autopsy.

## METHODS

This study was approved by the local ethics committee and followed the ethical guidelines of the Declaration of Helsinki. Data are stored in the REDCap electronic data capture tool<sup>15</sup> hosted at the University of Sao Paulo Medical School. Data access is available upon request to the corresponding author. Details of the methodology were previously published.<sup>16</sup>

## Selection of Subjects

In Brazil, an autopsy is mandatory in cases where the cause of death is unknown. The Sao Paulo Autopsy Service of the University of Sao Paulo performs around 14 000 autopsies a year and is the reference institution for identifying the causes of nontraumatic deaths in the metropolitan region of Sao Paulo.<sup>17</sup> Eligible subjects were selected prospectively between 2013 to 2015. The next of kin (NOK) of the deceased were invited by the team of nurses/gerontologists to participate in this study. The participants were asked to sign an informed consent form and respond to a semistructured interview.<sup>17</sup> The criteria for inclusion were: age at death of 30 years or older, postmortem interval of <24 hours, informed consent form accepted and signed by the NOK, and daily or weekly interaction between the NOK and the deceased at least 6 months before the death to provide accurate clinical data. Exclusion criteria were NOK unable to answer the questions of the semistructured interview, fixation of PvAT >72 hours prior, heart with signs of autolysis, heart disease attributable to local inflammation (eg hemopericardium, presence of a stent), previous cardiac surgery, immunosuppression by drugs/radiotherapy, autoimmune diseases, a

site with a myocardial bridge, and the presence of sepsis or systemic inflammation detected through biopsy of main organs.<sup>16</sup>

### Clinical Data Evaluation

We used the following demographic data: age at death, sex, race categorized as White or Black and Asian reported by the NOK and confirmed from the photograph on an official government document, level of education, and frequency of interaction between the NOK and the deceased.

The medical history included hypertension, diabetes, dyslipidemia, stroke, heart failure, smoking (never/previous or current), physical activity (domestic, work, or leisure physical activities at least 3 times a week), and alcohol consumption (never/previous or current). The presence of coronary artery disease was considered positive if the NOK reported a previous diagnosis of CAD, myocardial infarction, angioplasty, frequent chest pain, or coronary bypass surgery. We also investigated current and previous surgeries, medication, and other diseases.<sup>17</sup> The body mass index was calculated by direct measurements of height using a stadiometer and weight using an electronic scale, with the deceased in the supine position without clothes or shoes.

### Material Processing

Fresh hearts were collected and washed under running water, and the coronary arteries were filled with agar to avoid collapse. Next, the right coronary artery, trunk of the left coronary artery, left anterior descending artery, and left circumflex artery were dissected with 10 mm of surrounding PvAT. The PvAT was then removed from the coronary arteries at regular intervals of 15 mm and identified to match with the arterial segments. The PvAT was fixed by immersion in buffered paraformaldehyde at pH 7.2 to 7.4 for at least 24 hours and up to 72 hours, and the coronary arteries were immersed for at least 5 days. Next, both the PvAT and coronary artery fragments were immersed in paraffin, sliced lengthwise at 4  $\mu$ m intervals, and mounted on silanized slides (3-aminopropyl triethoxysilane; Sigma-Aldrich, St. Louis, MO).<sup>16</sup>

### Evaluation of Polarized Macrophages in the PvAT

Based on Hirata et al,<sup>9</sup> we identified M1 and M2 macrophages using an immunohistochemistry technique, as follows: (1) deparaffinization in hot xylene; (2) hydration with absolute, 95%, and 70% alcohol; (3) induction of antigenic recovery by heat in a pressure cooker with citric acid (10 mmol/L and pH 6.0); (4) blocking of endogenous peroxidase with a 3% hydrogen peroxide

10 volume; (5) incubation with primary antibodies diluted in phosphate buffer with 1% of bovine serum albumin at 4 °C overnight (M1 macrophages: rabbit monoclonal anti-C11c, EP1347Y, 1  $\mu$ L: 400  $\mu$ L; Abcam, Cambridge, United Kingdom) and (M2 macrophages: mouse monoclonal anti-CD206, 5C11, 1  $\mu$ L:1500  $\mu$ L; Abnova, Taiwan); (6) incubation with secondary antibody (Easylink One polymer HRP-conjugated streptavidin (HRP, horseradish peroxidase enzyme); EasyPath); (7) revelation with diaminobenzidine (Sigma-Aldrich, Steinheim, Germany); and (8) counter-staining with hematoxylin-eosin (Merck, Darmstadt, Germany). We used the pharyngeal tonsils as positive and negative control (Figure S1).<sup>16</sup>

The slides were scanned with Panoramic Scan (Panoramic Scan 250 Flash III; 3DHISTECH, Budapest, Hungary) and analyzed with a Panoramic Viewer virtual microscope (3DHISTECH), in which 20 fields, 600  $\mu$ m in diameter, were randomly distributed without magnification. The cells were counted by a rater (D.S.F.-I.) who was blinded to the identification of the coronary artery fragment.<sup>16</sup>

### Evaluation of Coronary Artery Atherosclerosis

During the macroscopic evaluation, one fragment was selected from each of the main arteries with signs of instability.<sup>18</sup> In the absence of plaque instability, we selected the greater luminal narrowing together with the periplaque PvAT. Additionally, one segment, distal to the plaques and without macroscopic atherosclerosis, was selected with the adjacent PvAT (control PvAT). These macroscopic segments were photographed with a stereomicroscope (SMZ 1000; Nikon, Tokyo, Japan). The segment was immersed in paraffin, cut in 4- $\mu$ m slices, and stained with hematoxylin-eosin, Masson's trichrome, and Verhoeff (Data S1).

We then photographed each stained slide. We created the software program using LabView ambience (Laboratory Virtual Instrumentation Engineering Workbench; National Instruments, Austin, TX) to evaluate the images of the coronary arteries. The atherosclerotic plaque analyzer (APA) aims to identify and delimit the components of the atherosclerotic plaque and other morphometric measurements using the photos of the stained slides. The APA gathers this information and propagates information from one stain to another. The APA can correct the background to remove shadows, localize the artery, calibrate the scale bar to real size, convert the scale bar to millimeters or micrometers, contour the lumen and internal elastic lamina in Verhoeff stain automatically,<sup>19</sup> and calculate the fibrous cap and IMT. All of these steps are performed automatically, then checked by the researcher. The APA calculates the percentage of arterial obstruction using

the formula: area delimited by the internal elastic lamina minus the area delimited by the lumen, divided by the area delimited by the internal elastic lamina, and then multiplied by 100.<sup>20</sup> The IMT was calculated by the distance between the lumen and the external elastic lamina.<sup>21</sup> We considered the mean distance throughout the circumference of the lesion. Fibrous cap thickness (FCT) was measured at the thinnest distance.<sup>22</sup> The APA also calculates the percentage of the plaque area that was occupied by the lipid core, necrotic core, calcifications, healed area, intraplaque hemorrhage, collagen, smooth muscle cell (SMC), and fibrous cap. We also counted the number of vasa vasorum in the 3 layers of the artery. These measurements were continuous variables. We validated the lumen and internal elastic lamina measured by the APA compared with the measurements of an experienced researcher (D.S.F.-I.). We found 94% agreement for the lumen (Figure S2A) and internal elastic lamina (Figure S2B). The atherosclerotic plaques were classified as stable or unstable (ie, luminal thrombosis/healed component of the previous thrombosis and intraplaque hemorrhage).<sup>18</sup>

### Statistical Analysis

The clinical and sociodemographic data were reported as average $\pm$ SD or median and interquartile interval, according to the variable distribution. The categorical variables were presented as absolute and relative frequencies. We compared the plaque composition according to thrombosis and hemorrhage status using regression models with robust SE for repeated measures in the same individual (4 arterial segments per person) using Huber-White sandwich estimators.<sup>23</sup> We considered, as dependent variables, the percentage of atherosclerotic plaque components and morphometric measures (continuous variable) and the instability classification (categorical variable). The independent variables were the densities of M1, M2, and the ratio of M1 to M2 macrophages in the periplaque PvAT (continuous variable).

We tested the correlation of atherosclerosis components and morphometric measures with macrophage densities, using linear regression with robust SE for repeated measures in the same individual when the regression residuals had Gaussian distribution. In cases where this assumption did not hold, we use the countfit analyses in Stata to identify which test would be more appropriate, Poisson's regression or negative binomial regression.<sup>24</sup> We also tested the association between the densities of polarized macrophages adjacent to stable and unstable atherosclerotic plaques, using logistic regression with robust SEs for repeated measures. We compared the macrophage densities between periplaque and control PvAT by subtracting the respective densities of these sites. The

association of these differences with atherosclerotic components and morphometric measurements was performed using the same models described above. We adjusted the models for age, sex, hypertension, diabetes, smoking, alcohol consumption, physical inactivity, and body mass index. We also tested the correlation of components of the atherosclerotic plaque and morphometric measurements with the densities of polarized macrophages stratified by plaque instability as sensitivity analyses. The Stata 16.0 (StataCorp, College Station, TX) and R (R Foundation for Statistical Computing, Vienna, Austria) programs were used to perform the statistical analyses. The  $\alpha$  level was 0.05 in 2-tailed tests.

## RESULTS

### Subjects

We collected 319 fragments of coronary atherosclerosis from 82 individuals. The mean age was 69.0 $\pm$ 14.4 years; 50% were women, 58% were White, and the median level of education was 4 years (interquartile range, 1–6 years). Hypertension (54%) and diabetes (36%) were the most common diseases. Only 12% of the individuals had received a previous diagnosis of CAD or stroke. The most prevalent cardiovascular risk factor was physical inactivity (68%) (Table S1).

### Coronary Atherosclerosis

The coronary artery had an average 54 $\pm$ 26% of lumen obstruction. We also observed a mean of 43 $\pm$ 23% arterial obstruction in stable plaques, 65 $\pm$ 16% in plaques with hemorrhage, and 99 $\pm$ 3% in plaques with thrombosis (Figure S3A). The average FCT was 24.7 $\pm$ 29.7  $\mu$ m in the thinnest portion (Figure S3C). The highest number of vasa vasorum was observed in the adventitia layer (Figure S3D through S3F). As for plaque composition, the most prevalent content was SMC, with an average of 33 $\pm$ 44% of the plaque area occupied by SMC, followed by lipid (23 $\pm$ 19%), collagen (22 $\pm$ 22%), fibrous cap (16 $\pm$ 9%), calcification (7 $\pm$ 15%), and necrosis (3 $\pm$ 11%) (Figure S4).

### Were Polarized Macrophages in the PvAT Correlated With Components of Atherosclerosis?

In the adjusted analysis, the M1 macrophage density in the periplaque PvAT was related to an increase in plaque size ( $\beta$ , 1.44 [95% CI, 0.33–2.54];  $P=0.01$ ) and IMT ( $\beta$ , 13.61 [95% CI, 2.06–25.17];  $P=0.02$ ). Also, the M1 macrophage density in the periplaque PvAT was related to a decrease in SMC area ( $\beta$ , –3.29 to –0.27;  $P=0.02$ ) and a decrease in FCT ( $\beta$ , –0.30 [95% CI, –0.59 to –0.01];  $P=0.03$ ) (Table 1).

**Table 1. Correlation of the M1 CD11c<sup>+</sup> Macrophage Density in the Periplaque Perivascular Adipose Tissue With Coronary Artery Atherosclerosis (n=319 Arterial Segments)**

M1 CD11c <sup>+</sup> macrophages density, cell 10 <sup>-5</sup> /μm <sup>2</sup>	Unadjusted model			Adjusted model*		
	Coefficient	95% CI	P value	Coefficient	95% CI	P value
Arterial obstruction, % <sup>†</sup>	1.56	0.63 to 2.49	0.001	1.44	0.33 to 2.54	0.01
IMT, μm <sup>†</sup>	15.40	4.67 to 26.13	0.005	13.61	2.06 to 25.17	0.02
Collagen, % <sup>†</sup>	0.55	-0.05 to 1.16	0.07	0.36	-0.39 to 1.12	0.33
Smooth muscle cell, % <sup>†</sup>	-2.11	-3.39 to -0.83	0.002	-1.78	-3.29 to -0.27	0.02
Fibrous cap, % <sup>†</sup>	-0.31	-0.56 to -0.06	0.01	-0.30	-0.59 to -0.01	0.03
Minimum FCT, μm <sup>†</sup>	0.03	-0.97 to 0.89	0.93	0.13	-0.80 to 1.08	0.76
Calcification, % <sup>‡</sup>	0.05	-0.00004 to 0.10	0.05	0.07	-0.01 to 0.16	0.11
Lipid, % <sup>†</sup>	0.66	-0.03 to 1.35	0.06	0.60	-0.20 to 1.41	0.14
Necrosis, % <sup>†</sup>	0.06	-0.05 to 0.18	0.29	0.02	-0.10 to 0.15	0.72
Intraplaque hemorrhage, % <sup>†</sup>	-0.07	-0.19 to 0.04	0.23	-0.002	-0.14 to 0.13	0.96
Vasa vasorum intima layer, n <sup>§</sup>	-0.04	-0.15 to 0.07	0.50	-0.05	-0.15 to 0.04	0.27
Vasa Vasorum media layer, n <sup>§</sup>	0.003	-0.08 to 0.09	0.94	-0.03	-0.11 to 0.05	0.46
Vasa vasorum adventitia layer, n <sup>§</sup>	0.01	-0.02 to 0.05	0.42	0.01	-0.02 to 0.06	0.43

FCT indicates fibrous cap thickness; and IMT, intima-media thickness.

\*Adjusted for age, sex, hypertension, diabetes, body mass index, physical inactivity, alcohol use, and smoking.

<sup>†</sup>Linear regression with SE adjusted for repeated measures in the same individual.

<sup>‡</sup>Negative binomial regression with SE adjusted for repeated measures in the same individual.

<sup>§</sup>Poisson regression with SE adjusted for repeated measures in the same individual.

Similarly, M2 macrophage density in the periplaque PvAT was associated with arterial obstruction in the coronary arteries ( $\beta$ , 0.77 [95% CI, 0.12–1.42];  $P=0.02$ ) and IMT ( $\beta$ , 9.09 [95% CI, 1.54–16.63];  $P=0.01$ ). The increase in M2 macrophage density in the periplaque PvAT was also correlated with an increase in plaque calcification ( $\beta$ , 0.09 [95% CI, 0.01–0.18];  $P=0.03$ ) (Table S2).

The M1/M2 ratio, which identifies the more frequent inflammatory profile, showed that M1 was more frequent than M2 in the presence of arterial obstruction. Each increase in the M1/M2 ratio was related to an average 9% increase in arterial obstruction ( $\beta$ , 9.15 [95% CI, 1.44–16.87];  $P=0.02$ ). In addition, the increase of proinflammatory state in the periplaque PvAT was correlated with a higher lipid content in the atherosclerotic plaque ( $\beta$ , 6.89 [95% CI, 1.14–12.64];  $P=0.01$ ) and a higher number of vasa vasorum in the adventitia layer ( $\beta$ , 0.29 [95% CI, 0.05–0.53];  $P=0.01$ ). On the other hand, the proinflammatory state was related to a decrease in SMC content ( $\beta$ , -12.25 [95% CI, -22.88 to -1.62];  $P=0.02$ ) (Table 2).

### Were Polarized Macrophages in the Pericoronary PvAT Associated With Unstable Atherosclerotic Plaques?

A greater density of M1 proinflammatory macrophages in the periplaque PvAT was associated with an increased risk of thrombosis (odds ratio [OR], 1.11 [95% CI, 1.10–1.23];  $P=0.03$ ) (Figure, Table S3). Corroborating

this finding, the proinflammatory profile was predominant over anti-inflammatory macrophages. For each unit increase in M1/M2 ratio, there was a 1.95 times higher risk of thrombosis (OR, 1.95 [95% CI, 1.05–3.61];  $P=0.03$ ) (Figure, Table S3). In atherosclerotic plaques with thrombus, the M1 macrophage density in the periplaque PvAT ( $\beta$ , 0.02 [95% CI, 0.01–0.07];  $P=0.02$ ) and the M1/M2 ratio density in the periplaque PvAT ( $\beta$ , 0.30 [95% CI, 0.12–0.49];  $P=0.001$ ) were associated with an increase in the number of vasa vasorum in the adventitia layer. Additionally, in plaques with thrombus, the increase in the number of vasa vasorum in the adventitia layer was associated with a decrease in the number of M2 macrophages ( $\beta$ , -0.03 [95% CI, -0.05 to -0.01];  $P=0.003$ ). Alternatively, there was no association between intraplaque hemorrhage in the coronary arteries and the density of M1 and M2 macrophages in the periplaque PvAT, or with the M1/M2 ratio (Figure S5, Table S3).

### Are These Associations Only Adjacent to Atherosclerotic Plaques, or Are They Diffusely Distributed in the Cardiac Fat?

When the difference in macrophage densities between the periplaque PvAT and the control PvAT is large, this means that the macrophage density in the periplaque PvAT is greater than in the control PvAT in the same individual. A greater M1 difference was correlated with greater collagen content in atherosclerotic plaques ( $\beta$ , 0.92 [95% CI, 0.05–1.78];  $P=0.03$ ) (Figure S6). We

**Table 2. Correlation Between M1 CD11c<sup>+</sup>/M2 CD206<sup>+</sup> Macrophage Ratio in the Periplaque Perivascular Adipose Tissue With Coronary Artery Atherosclerosis (n=319 Arterial Segments)**

Ratio of M1 CD11c <sup>+</sup> / M2 CD206 <sup>+</sup> macrophages density, cell 10 <sup>-5</sup> /μm <sup>2</sup>	Unadjusted model			Adjusted model*		
	Coefficient	95% CI	P value	Coefficient	95% CI	P value
Arterial obstruction, % <sup>†</sup>	8.30	0.80 to 15.80	0.03	9.15	1.44 to 16.87	0.02
IMT, μm <sup>†</sup>	51.52	-32.92 to 135.97	0.22	64.21	-21.07 to 149.50	0.13
Collagen, % <sup>†</sup>	2.30	-2.60 to 7.22	0.35	3.56	-2.12 to 9.24	0.21
Smooth muscle cell, % <sup>†</sup>	-9.64	-19.6 to 0.39	0.06	-12.25	-22.88 to -1.62	0.02
Fibrous cap, % <sup>†</sup>	-2.78	-4.68 to -0.88	0.005	-2.98	-5.06 to -0.89	0.006
Minimum FCT, μm <sup>†</sup>	2.01	-4.99 to 9.02	0.56	2.14	-5.39 to 9.69	0.57
Calcification, % <sup>‡</sup>	0.31	-0.33 to 0.97	0.34	0.21	-0.57 to 1.01	0.58
Lipid, % <sup>†</sup>	6.15	0.87 to 11.43	0.02	6.89	1.14 to 12.64	0.01
Necrosis, % <sup>‡</sup>	0.02	-1.02 to 1.06	0.96	-0.35	-1.37 to 0.66	0.49
Intraplaque hemorrhage, % <sup>‡</sup>	-0.54	-1.49 to 0.39	0.25	-0.30	-0.99 to 0.38	0.38
Vasa vasorum intima layer, n <sup>§</sup>	0.005	-0.69 to 0.70	0.98	-0.01	-0.62 to 0.58	0.95
Vasa Vasorum media layer, n <sup>§</sup>	-0.09	-0.82 to 0.62	0.78	-0.07	-0.82 to 0.66	0.83
Vasa vasorum adventitia layer, n <sup>§</sup>	0.24	0.01 to 0.47	0.03	0.29	0.05 to 0.53	0.01

FCT indicates fibrous cap thickness; and IMT, intima-media thickness.

\*Adjusted for age, sex, hypertension, diabetes, body mass index, physical inactivity, alcohol consumption, and smoking.

<sup>†</sup>Linear regression with SE adjusted for repeated measures in the same individual.

<sup>‡</sup>Negative binomial regression with SE adjusted for repeated measures in the same individual.

<sup>§</sup>Poisson regression with SE adjusted for repeated measures in the same individual.

found no differences between M1 macrophages in the periplaque and control PvAT in association with other coronary atherosclerosis components (Figure S7). Additionally, we found no differences between M2 macrophages in the periplaque and control PvAT in association with coronary atherosclerosis components (Figure S8). However, greater M2 macrophage density difference was related to greater IMT ( $\beta$ , 11.76 [95% CI, 1.43–22.09];  $P=0.02$ ) and to a decrease in the number of vasa vasorum in the adventitia layer ( $\beta$ , -0.03 [95% CI, -0.05 to -0.005];  $P=0.01$ ) (Figure S9).

### Is There a Difference in the Association Between the Density of Polarized Macrophages in the PvAT and Atherosclerotic Components According to the Presence of Thrombosis?

In the atherosclerotic plaques with thrombosis, only M1 macrophage associations were significant. The increase in M1 macrophage density in the periplaque PvAT was related to a decrease in fibrous cap area ( $\beta$ , -1.03 [95% CI, -1.99 to -0.08];  $P=0.03$ ) and an increase in the number of vasa vasorum in the adventitia layer ( $\beta$ , 0.03 [95% CI, 0.01–0.07];  $P=0.02$ ) (Table 3). In atherosclerotic plaques without thrombosis, most associations with M2 macrophages were significant and were associated with greater arterial obstruction ( $\beta$ , 0.69 [95% CI, 0.11–1.27];  $P=0.01$ ), greater calcification ( $\beta$ , 0.10 [95% CI, 0.01–0.19];  $P=0.02$ ), and greater

necrosis content ( $\beta$ , 0.20 [95% CI, 0.01–0.38];  $P=0.03$ ). The only association found in plaques with thrombosis was a decrease in the number of vasa vasorum in the adventitia layer ( $\beta$ , -0.003 [95% CI, -0.05 to -0.01];  $P=0.003$ ) (Table 4).

The proinflammatory state was predominantly associated with components and measurements in plaques with thrombosis. The greater M1/M2 macrophages ratio was associated with a decrease in FCT ( $\beta$ , -6.18 [95% CI, -10.39 to -1.97];  $P=0.006$ ), an increase in lipid content ( $\beta$ , 11.07 [95% CI, 3.25–18.88];  $P=0.008$ ), and an increase in the number of vasa vasorum in the adventitial layer ( $\beta$ , 0.30 [95% CI, 0.12–0.49];  $P=0.001$ ). On the other hand, a proinflammatory state was associated with a smaller necrosis content ( $\beta$ , -3.45 [95% CI, -6.41 to -0.50];  $P=0.02$ ) (Table 5).

## DISCUSSION

Coronary atherosclerosis was mainly associated with proinflammatory macrophages in the periplaque PvAT. M1 macrophages in the periplaque PvAT were correlated with an increase in plaque size, lipid content, and the number of vasa vasorum in the adventitia layer, and with a decrease in SMC content in the atherosclerotic plaques. Also, M2 macrophages in the periplaque PvAT were correlated with an increase in plaque size and calcification content. As for differences in the density of polarized macrophages in the periplaque PvAT and the control PvAT, we found that M1 macrophages

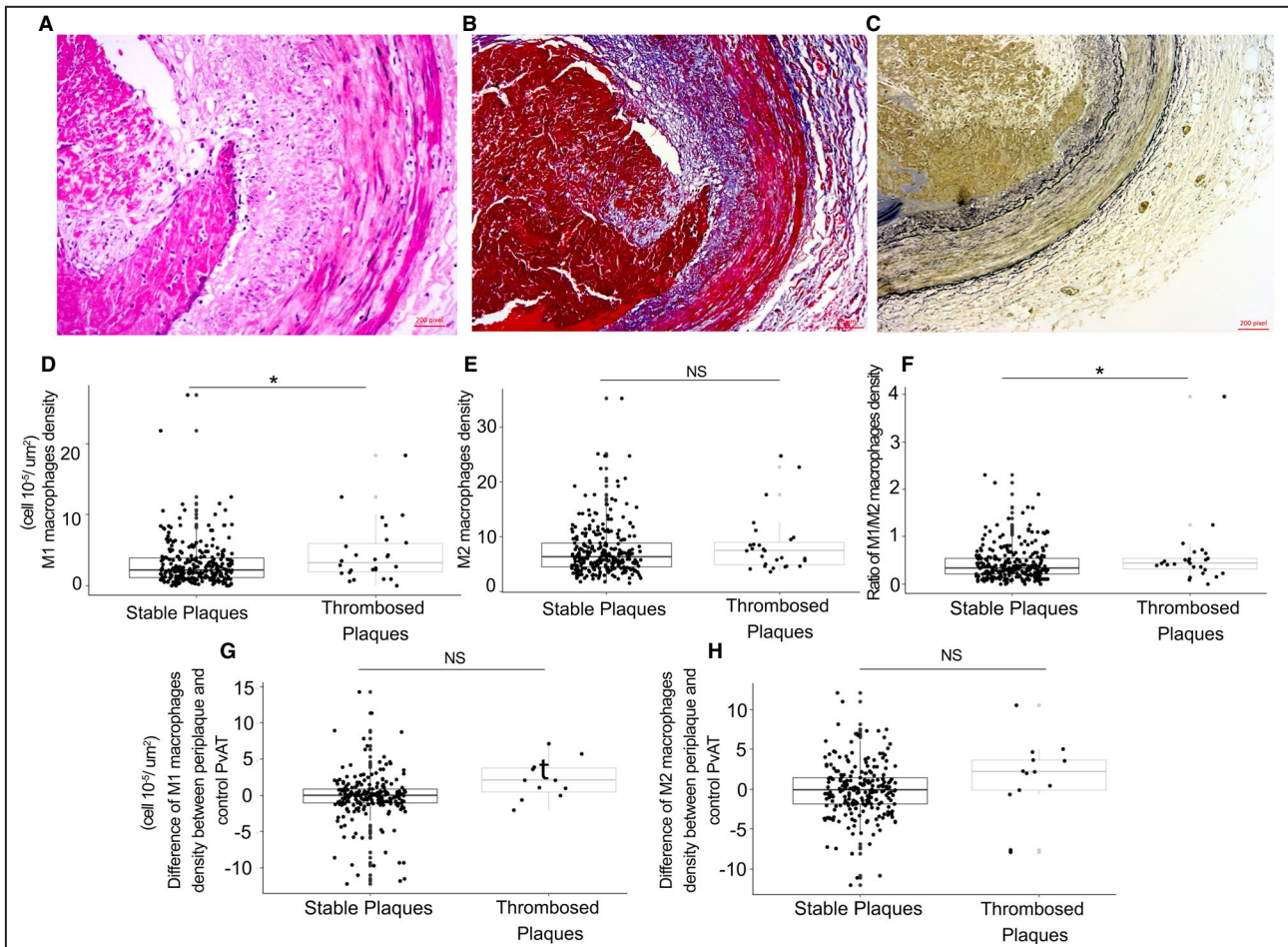


**Figure.** Association between the polarized macrophage density in the periplaque perivascular adipose tissue (PvAT) and unstable atherosclerotic plaques (n=319 arterial segments).

**A**, Atherosclerotic plaque with the presence of thrombus, hematoxylin-eosin stain. **B**, Atherosclerotic plaque with the presence of thrombus, Masson's Trichrome stain. **C**, Atherosclerotic plaque with the presence of thrombus, Verhoeff stain. **D** through **H**, Association between the density of polarized macrophages in the periplaque PvAT and atherosclerotic plaques with thrombosis. Linear regression adjusted for repeated measures in the same individual and confounding factors. \*, significant result. NS, non-significant result.

in the periplaque PvAT were associated with greater collagen content, whereas M2 macrophages in the periplaque PvAT were related to greater IMT. The M1/M2 ratio showed a predominance of the proinflammatory over the anti-inflammatory profile. Additionally, M1 macrophage density in the periplaque PvAT was associated with an increased risk of coronary thrombosis. M1 macrophages were related to characteristics of atherosclerotic plaque destabilization, such as an increase in lipid content and the number of vasa vasorum, and a decrease in the necrotic content and FCT. In contrast, the anti-inflammatory macrophage profile was predominant in plaques without thrombosis and was associated with an increase in arterial obstruction, calcification, and necrotic content.

We found that the atherosclerosis development was associated with macrophages that expressed a proinflammatory profile, whereas the anti-inflammatory profile was related to plaque stabilization. Our results

are in agreement with previous studies with human biopsy samples that found a predominance of proinflammatory macrophages in patients with CAD.<sup>7-10</sup> Only one study did not find any difference in the number of polarized macrophages between patients with CAD and controls, which could be explained by the differences in sample size and the number of analyzed fields quantified.<sup>11</sup> Similarly, studies in animal models found an increase in plaque size, IMT, and lipid content in the presence of macrophages. Moreover, the transplantation of visceral PvAT next to carotid arteries led to a higher macrophage concentration adjacent to the transplanted area.<sup>5</sup> Also, in animal models, this leukocyte infiltration in the PvAT seems to precede atherosclerosis development and atherosclerotic vascular dysfunction, because in early plaques, a greater density of M1 macrophages in the PvAT was found in knockout apoE (apolipoprotein E)-deficient mice.<sup>6</sup>

**Table 3. Comparison of M1 CD11c<sup>+</sup> Macrophage Densities in the Periplaque Perivascular Adipose Tissue Adjacent to Segments With and Without Thrombosis (n=319 Arterial Segments)**

Macrophages M1 CD11c <sup>+</sup> density, cell 10 <sup>-5</sup> /μm <sup>2</sup>	Without thrombus, n=292 coronary plaques			Thrombus, n=27 coronary plaques		
	Adjusted model*			Adjusted model*		
	Coefficient	95% CI	P value	Coefficient	95% CI	P value
Arterial obstruction, % <sup>†</sup>	0.95	-0.003 to 1.91	0.05	-0.29	-0.83 to 0.25	0.28
IMT, μm <sup>†</sup>	10.09	-2.84 to 23.03	0.12	2.99	-42.45 to 48.43	0.89
Collagen, % <sup>†</sup>	0.18	-0.56 to 0.94	0.61	-0.23	-2.16 to 1.68	0.80
Smooth muscle cell, % <sup>†</sup>	-1.31	-2.86 to 0.23	0.09	‡	‡	
Fibrous cap, % <sup>†</sup>	-0.22	-0.49 to 0.04	0.10	-1.03	-1.99 to -0.08	0.03
Minimum FCT, μm <sup>†</sup>	0.30	-0.93 to 1.53	0.62	-1.02	-2.44 to 0.40	0.15
Calcification, % <sup>§</sup>	0.06	-0.02 to 0.15	0.18	0.07	-0.32 to 0.48	0.70
Lipid, % <sup>†</sup>	0.27	-0.38 to 0.94	0.40	1.78	-0.66 to 4.24	0.14
Necrosis, % <sup>§</sup>	0.09	-0.05 to 0.24	0.22	-0.13	-0.67 to 0.40	0.61
Intraplaque hemorrhage, % <sup>§</sup>	-0.09	-0.25 to 0.06	0.23	-0.01	-0.09 to 0.07	0.81
Vasa vasorum intima layer, n <sup>  </sup>	-0.06	-0.17 to 0.05	0.28	-0.10	-0.22 to 0.01	0.09
Vasa Vasorum media layer, n <sup>  </sup>	-0.03	-0.15 to 0.08	0.56	-0.09	-0.25 to 0.07	0.28
Vasa vasorum adventitia layer, n <sup>  </sup>	-0.008	-0.03 to 0.02	0.60	0.03	0.01 to 0.07	0.02

FCT indicates fibrous cap thickness; and IMT, intima-media thickness.

\*Adjusted for age, sex, hypertension, diabetes, body mass index, physical inactivity, alcohol consumption, and smoking.

<sup>†</sup>Linear regression with SE adjusted for repeated measures in the same individual.

<sup>‡</sup>Absence of observations.

<sup>§</sup>Negative binomial regression with SE adjusted for repeated measures in the same individual.

<sup>||</sup>Poisson regression with SE adjusted for repeated measures in the same individual.

Likewise, M2 macrophages in the PvAT were also associated with atherosclerosis in our study. Previously, M2 macrophage density in the PvAT was greater in patients with CAD,<sup>8,9</sup> whereas another study did not corroborate this finding.<sup>10</sup> Similar to our results that showed that an increase in M2 macrophage density was correlated with an increase in plaque size and calcification, other imaging studies found an association between PvAT volume and coronary artery calcification.<sup>25-27</sup> Moreover, macrophage infiltration and neoangiogenesis in the epicardial adipose tissue were associated with mild coronary calcification; however, macrophage polarization was not assessed.<sup>28</sup> In atherosclerotic plaques, M2 macrophages seem to play a role in inflammation resolution through macrocalcification.<sup>29,30</sup> Although microcalcification is considered a proinflammatory process, macrocalcification in atherosclerosis is a signal of plaque stabilization by phagocytosis, resulting in necrotic cellular debris and apoptotic cell resolution. M2 macrophages were also related to the production of the extracellular matrix, osteoblastic differentiation, and maturation of vascular SMC.<sup>29</sup>

Although we found that periplaque PvAT inflammation was related to greater collagen content and IMT, and a fewer number of vasa vasorum compared with the control PvAT, another study did not find any difference.<sup>31</sup> This discrepancy could be explained by the different sample sizes, the number of quantified fields of the PvAT, the different immunohistochemistry techniques

used, and the different statistical approaches in terms of adjustment for possible confounders. Imaging studies have already shown a greater density of immune cells surrounding culprit lesions in patients with acute coronary syndrome.<sup>32</sup> Therefore, PvAT inflammation may be heterogeneous in the same individual with bidirectional activity between the arterial wall and the periplaque PvAT in humans.<sup>33,34</sup> On the other hand, in animal models, it appears that early leukocyte infiltration in the PvAT occurs before the artery wall inflammation and endothelial dysfunction,<sup>6</sup> suggesting a causal effect of PvAT in endothelial dysfunction.<sup>5</sup> Also, in animal models, removal of the PvAT in the proximal left anterior descending artery reduced the percentage of stenosis compared with controls 3 months after surgery, whereas in the control group, there was an increase in the stenosis index.<sup>35</sup>

Macrophages in the PvAT were previously associated with an increased risk of thrombosis in human coronary arteries.<sup>13</sup> Greater PvAT attenuation, which is a marker of PvAT inflammation in imaging exams, was independently associated with poorer global coronary reserve flow 1 month after an acute coronary event,<sup>36</sup> higher acute coronary syndrome,<sup>37</sup> and increased cardiac death.<sup>38</sup> Our stratified analyses demonstrated that the inflammation mediated by M1 macrophages in the periplaque PvAT was associated with characteristics of plaque progression and destabilization in thrombosed coronary arteries, suggesting that M1 macrophages in



**Table 4. Comparison of M2 CD206<sup>+</sup> Macrophage Densities in the Periplaque Perivascular Adipose Tissue Adjacent to Segments With and Without Thrombosis (n=319 Arterial Segments)**

Macrophages M2 CD11c <sup>+</sup> density, cell 10 <sup>-5</sup> /μm <sup>2</sup>	Without thrombus, n=292 coronary plaques			Thrombus, n=27 coronary plaques		
	Adjusted model*			Adjusted model*		
	Coefficient	95% CI	P value	Coefficient	95% CI	P value
Arterial obstruction, % <sup>†</sup>	0.69	0.11 to 1.27	0.01	-0.25	-0.64 to 0.12	0.17
IMT, μ <sup>†</sup>	8.41	0.03 to 16.80	0.049	6.19	-16.95 to 29.33	0.58
Collagen, % <sup>†</sup>	0.004	-0.63 to 0.64	0.98	-0.50	-1.74 to 0.73	0.40
Smooth muscle cell, % <sup>†</sup>	-0.67	-1.89 to 0.54	0.27	‡	‡	
Fibrous cap, % <sup>†</sup>	0.06	-0.22 to 0.36	0.64	-0.34	-1.21 to 0.51	0.41
Minimum FCT, μm <sup>§</sup>	-0.44	-1.21 to 0.32	0.25	-0.19	-1.22 to 0.83	0.70
Calcification, % <sup>§</sup>	0.10	0.01 to 0.19	0.02	0.10	-0.21 to 0.42	0.51
Lipid, % <sup>†</sup>	0.14	-0.31 to 0.60	0.53	0.42	-1.19 to 2.05	0.59
Necrosis, % <sup>§</sup>	0.20	0.01 to 0.38	0.03	0.12	-0.14 to 0.39	0.35
Intraplaque hemorrhage, % <sup>§</sup>	0.00001	-0.14 to 0.14	1.00	0.03	-0.06 to 0.12	0.49
Vasa vasorum intima layer, n <sup>  </sup>	-0.05	-0.13 to 0.02	0.15	-0.06	-0.14 to 0.02	0.16
Vasa vasorum media layer, n <sup>  </sup>	-0.08	-0.17 to 0.01	0.09	0.02	-0.10 to 0.16	0.70
Vasa vasorum adventitia layer, n <sup>  </sup>	-0.006	-0.03 to 0.01	0.61	-0.03	-0.05 to -0.01	0.003

FCT indicates fibrous cap thickness; and IMT, intima-media thickness.

\*Adjusted for age, sex, hypertension, diabetes, body mass index, physical inactivity, alcohol consumption, and smoking.

<sup>†</sup>Linear regression with SE adjusted for repeated measures in the same individual.

<sup>‡</sup>Absence of observations.

<sup>§</sup>Negative binomial regression with SE adjusted for repeated measures in the same individual.

<sup>||</sup>Poisson regression with SE adjusted for repeated measures in the same individual.

the PvAT might influence the inflammation in acute coronary events. Accordingly, unstable lesions in human carotid arteries had a higher concentration of M1 macrophages, and metalloproteinases-2 and 9 compared with stable plaques.<sup>39</sup> In this way, either M1 macrophages in the PvAT or their cytokine production could contribute to plaque destabilization. We also found that M2 macrophages in the periplaque PvAT may play a role mainly in stable plaques, by the association with calcium and necrosis in stable plaques. These results are in line with those reported in the literature, in which stable atherosclerotic plaques had a greater concentration of M2 macrophages.<sup>39</sup>

The increase in the number of vasa vasorum in the adventitia layer was associated with an increase in the M1/M2 ratio density in the periplaque PvAT. A similar finding was observed in atherosclerotic plaques with thrombus both for the M1 macrophage density and for M1/M2 ratio density in the periplaque PvAT. Additionally, in plaques with thrombus, the increase in the number of vasa vasorum in the adventitia layer was related to a decrease in the number of M2 macrophages. These findings suggest that an increase in the number of vasa vasorum could be the link between the proinflammatory profile in the PvAT, coronary atherosclerosis, and plaque destabilization. Experimental studies in mice demonstrated that the neoangiogenesis induction increased the number of macrophages in the perivascular area before atherosclerotic plaque

formation and promoted a faster plaque progression.<sup>40</sup> Our findings are in line with a recent study using autopsy material. However, some methodological differences with our study are present; in the other study they did not evaluate unstable plaques, the inflammation in the PvAT was detected by molecule expression analyses, and the plaque composition was measured by intravascular ultrasound.<sup>41</sup> It is also suggested that vasa vasorum promotes vasospasm through the PvAT and artery inflammation by activation of the paracrine pathway.<sup>42</sup> These findings suggested a possible role of adventitia vasa vasorum in the migration of inflammatory cells from the periplaque PvAT to the atherosclerotic plaque.

Our results should be interpreted considering some limitations. First, because it is an observational cross-sectional study, we cannot establish causality relationships. Second, it is important to consider that macrophage polarization in vivo has a large plasticity that can be modified by signaling changes from the atherosclerotic plaques and periplaque PvAT.<sup>43,44</sup> Thus, the classification of M1 CD11c<sup>+</sup> macrophages and M2 CD206<sup>+</sup> macrophages could be simplistic, because it represents the extremes of macrophage polarization. Further studies in animals and humans are needed to identify other markers of macrophage transition. Additionally, we did not evaluate cytokines and adipocytokines in the PvAT or the macrophage polarization in the coronary artery plaques. Moreover,

**Table 5. Comparison of the Ratio Between M1 CD11c<sup>+</sup>/M2 CD206<sup>+</sup> Macrophage Densities in the Periplaque Perivascular Adipose Tissue Adjacent to Segments With and Without Thrombosis (n=319 Arterial Segments)**

Ratio M1 CD11c <sup>+</sup> /M2 density, cell 10 <sup>-5</sup> /μm <sup>2</sup>	Without thrombus, n=292 coronary plaques			Thrombus, n=27 coronary plaques		
	Adjusted model*			Adjusted model*		
	Coefficient	95% CI	P value	Coefficient	95% CI	P value
Arterial obstruction, % <sup>†</sup>	6.08	-2.03 to 14.19	0.14	-0.39	-1.40 to 0.61	0.42
IMT, μm <sup>†</sup>	33.43	-72.82 to 139.69	0.53	-33.59	-246.67 to 179.48	0.74
Collagen, % <sup>†</sup>	2.83	-4.42 to 10.09	0.43	1.14	-5.58 to 7.86	0.72
Smooth muscle cell, % <sup>†</sup>	-9.35	-22.90 to 4.18	0.17	‡	‡	
Fibrous cap, % <sup>†</sup>	-2.37	-5.35 to 0.60	0.11	-4.71	-10.27 to 0.84	0.09
Minimum FCT, μm <sup>§</sup>	4.46	-6.98 to 15.92	0.43	-6.18	-10.39 to -1.97	0.006
Calcification, % <sup>§</sup>	0.03	-0.83 to 0.90	0.93	-0.39	-1.59 to 0.80	0.51
Lipid, % <sup>†</sup>	3.58	-3.21 to 10.37	0.29	11.07	3.25 to 18.88	0.008
Necrosis, % <sup>§</sup>	-0.21	-1.04 to 0.61	0.60	-3.45	-6.41 to -0.50	0.02
Intraplaque hemorrhage, % <sup>§</sup>	-0.66	-1.98 to 0.65	0.32	-0.14	-0.41 to 0.12	0.29
Vasa vasorum intima layer, n <sup>  </sup>	0.20	-0.69 to 1.10	0.65	-0.23	-0.55 to 0.07	0.13
Vasa vasorum media layer, n <sup>  </sup>	0.17	-0.73 to 1.08	0.70	-1.43	-5.22 to 2.35	0.45
Vasa vasorum adventitia layer, n <sup>  </sup>	0.06	-0.22 to 0.35	0.64	0.30	0.12 to 0.49	0.001

FCT indicates fibrous cap thickness; and IMT, intima-media thickness.

\*Adjusted for age, sex, hypertension, diabetes, body mass index, physical inactivity, alcohol consumption, and smoking.

<sup>†</sup>Linear regression with SE adjusted for repeated measures in the same individual.

<sup>‡</sup>Absence of observations.

<sup>§</sup>Negative binomial regression with SE adjusted for repeated measures in the same individual.

<sup>||</sup>Poisson regression with SE adjusted for repeated measures in the same individual.

the lack of follow-up of subjects in this study did not allow us to measure the clinical data directly. The search for clinical data in medical records was not an option because of the decentralization of public health in Brazil. However, information was collected with a reliable NOK, and 80% of them had lived with the deceased in the 6 months before death. Also, our semi-structured interview had higher levels of sensitivity and specificity.<sup>17,45,46</sup>

Our study also has several strengths. Although previous human studies compared CAD and control patients, the differences in our study design should be highlighted. We evaluated a range of plaque severity (early, vulnerable, stable, and unstable) using morphometric measurements.<sup>18</sup> The PESA (Progression of Early Subclinical Atherosclerosis) imaging study reinforced the importance of considering the early stages of atherosclerosis, because frequent vascular inflammation was found in asymptomatic middle-aged individuals with subclinical atherosclerosis, and even in 11% of the artery walls without atherosclerosis.<sup>47</sup> Additionally, we performed a careful statistical analysis considering repeated measures in the same individual and adjustment for possible confounders. Other strengths of the present study included the histopathological evaluation of all of the coronary arteries, and the collection of the fragments with the most severe

atherosclerosis and one control segment in the same individual. This comprehensive evaluation is only possible in autopsy studies, which are being conducted on a smaller scale every year worldwide. Moreover, both macrophage polarization and coronary atherosclerosis were measured directly, avoiding measurement bias. Additionally, we developed an imaging processing software that measured the components of coronary plaque and other measurements such as the percentage of arterial obstruction and FCT.<sup>19</sup> To the best of our knowledge, this is the first study to investigate the association between macrophage polarization in the PvAT and direct measures of plaque components of atherosclerosis in the coronary arteries. The findings of this study provide translational knowledge from animal models to humans. Animal models have several advantages, but they also have some limitations on the characteristics of the atherosclerotic plaques compared with those in humans. Intraplaque hemorrhage and neovascularization are rare in mice, plaque rupture is also rare in pigs, and the site of the lesions in rabbits is different than in humans.<sup>48</sup> This study therefore brings some insights into how polarized macrophages in the PvAT can cause coronary atherosclerosis for future investigations. Some randomized clinical trials on this topic are currently under investigation. The CANTOS (Canakinumab Anti-inflammatory

Thrombosis Outcomes Study) trial is investigating the anti-inflammatory agent canakinumab that acts in the IL-1 $\beta$  (interleukin-1 $\beta$ ), which has a role in macrophage polarization.<sup>49</sup> Also, the COLCOT (Colchicine Cardiovascular Outcomes Trial) is investigating colchicine, which suppresses the inflammasome and decrease levels of IL-1 $\beta$  and IL-18 (interleukin-18).<sup>50</sup>

In conclusion, the proinflammatory M1 macrophage profile in the periplateau PvAT was correlated with plaque progression and destabilization. Additionally, M1 macrophages in the periplateau PvAT were associated with a higher risk of coronary thrombosis. Anti-inflammatory M2 macrophages in the periplateau PvAT were correlated with plaque size, increased calcification and necrotic content, and decreased the number of vasa vasorum in the adventitia layer. We did not find any associations between the density of polarized macrophages in the periplateau PvAT and intraplaque hemorrhage.

## ARTICLE INFORMATION

Received July 16, 2021; accepted December 21, 2021.

### Affiliations

Department of Pathology (D.S.F.-I., C.A.P., L.F.d.S., M.Y.-E., R.E.P. L., C.K.S.) and Heart Institute (InCor) (S.H.G.L.), and Discipline of Geriatrics (C.K.S.), University of Sao Paulo Medical School, Sao Paulo, Brazil, University of Sao Paulo Medical School, Sao Paulo, Brazil; and Control and Automation Engineering, Federal Institute of Education, Science and Technology of Sao Paulo, Sao Paulo, Brazil (R.A.d.A., A.B.C.).

### Acknowledgments

The authors acknowledge K. C. S. Bispo and C. Arruda for their support in the execution of the histological techniques, and A. Gomes for her support in the execution of the immunohistochemical techniques.

### Sources of Funding

This study was supported by a research grant from the São Paulo Research Foundation (FAPESP) (2013/00335-2, 2017/11313-0). D.S.F.-I. received a scholarship from FAPESP (2013/12290-3, 2017/24066-1).

### Disclosures

The authors declare no conflicts of interest.

### Supplemental Material

Data S1  
Tables S1–S3  
Figures S1–S9

## REFERENCES

- World Health Organization. Cardiovascular diseases (CVDs). 2021. Available at: [https://www.who.int/en/news-room/fact-sheets/detail/cardiovascular-diseases-\(cvds\)](https://www.who.int/en/news-room/fact-sheets/detail/cardiovascular-diseases-(cvds)). Accessed November 16, 2021.
- Virani SS, Alonso A, Aparicio HJ, Benjamin EJ, Bittencourt MS, Callaway CW, Carson AP, Chamberlain AM, Cheng S, Dellings FN, et al. Heart disease and stroke statistics-2021 update: a report from the American Heart Association. *Circulation*. 2021;143:e254–e743. doi: 10.1161/CIR.0000000000000950
- Libby P, Hansson GK. Inflammation and immunity in diseases of the arterial tree: players and layers. *Circ Res*. 2015;116:307–311. doi: 10.1161/CIRCRESAHA.116.301313
- Chatterjee TK, Stoll LL, Denning GM, Harrelson A, Blomkalns AL, Idelman G, Rothenberg FG, Neltner B, Romig-Martin SA, Dickson EW, et al. Proinflammatory phenotype of perivascular adipocytes: influence

- of high-fat feeding. *Circ Res*. 2009;104:541–549. doi: 10.1161/CIRCRESAHA.108.182998
- Öhman MK, Luo W, Wang H, Guo C, Abdallah W, Russo HM, Eitzman DT. Perivascular visceral adipose tissue induces atherosclerosis in apolipoprotein E deficient mice. *Atherosclerosis*. 2011;219:33–39. doi: 10.1016/j.atherosclerosis.2011.07.012
- Skiba DS, Nosalski R, Mikolajczyk TP, Siedlinski M, Rios FJ, Montezano AC, Jawien J, Olszanecki R, Korbut R, Czesnikiewicz-Guzik M, et al. Anti-atherosclerotic effect of the angiotensin 1–7 mimetic AVE0991 is mediated by inhibition of perivascular and plaque inflammation in early atherosclerosis. *Br J Pharmacol*. 2017;174:4055–4069. doi: 10.1111/bph.13685
- Pierzynová A, Šrámek J, Cinkajzlová A, Kratochvílová H, Lindner J, Haluzík M, Kučera T. The number and phenotype of myocardial and adipose tissue CD68+ cells is associated with cardiovascular and metabolic disease in heart surgery patients. *Nutr Metab Cardiovasc Dis*. 2019;29:946–955. doi: 10.1016/j.numecd.2019.05.063
- Shimabukuro M, Hirata Y, Tabata M, Dagvasumberel M, Sato H, Kurobe H, Fukuda D, Soeki T, Kitagawa T, Takahashi S, et al. Epicardial adipose tissue volume and adipocytokine imbalance are strongly linked to human coronary atherosclerosis. *Arterioscler Thromb Vasc Biol*. 2013;33:1077–1084. doi: 10.1161/ATVBAHA.112.300829
- Hirata Y, Tabata M, Kurobe H, Motoki T, Akaike M, Nishio C, Higashida M, Mikasa H, Nakaya Y, Takahashi S, et al. Coronary atherosclerosis is associated with macrophage polarization in epicardial adipose tissue. *J Am Coll Cardiol*. 2011;58:248–255. doi: 10.1016/j.jacc.2011.01.048
- Gurses KM, Ozmen F, Kocyigit D, Yersal N, Bilgic E, Kaya E, Kopru CZ, Soyalt T, Doganci S, Tokgozoglu L, et al. Netrin-1 is associated with macrophage infiltration and polarization in human epicardial adipose tissue in coronary artery disease. *J Cardiol*. 2017;69:851–858. doi: 10.1016/j.jcc.2016.08.016
- Fitzgibbons TP, Lee N, Tran K-V, Nicoloso S, Kelly M, Tam SKC, Czech MP. Coronary disease is not associated with robust alterations in inflammation gene expression in human epicardial fat. *JCI Insight*. 2019;4:e124859. doi: 10.1172/jci.insight.124859
- Mikami T, Furuhashi M, Sakai A, Numaguchi R, Harada R, Naraoka S, Kamada T, Higashiura Y, Tanaka M, Ohori S, et al. Antiatherosclerotic phenotype of perivascular adipose tissue surrounding the saphenous vein in coronary artery bypass grafting. *J Am Heart Assoc*. 2021;10:18905. doi: 10.1161/JAHA.120.018905
- Farias-Itao DS, Pasqualucci CA, Nishizawa A, da Silva LFF, Campos FM, Bittencourt MS, da Silva KCS, Leite REP, Grinberg LT, Ferretti-Rebustini REDL, et al. B lymphocytes and macrophages in the perivascular adipose tissue are associated with coronary atherosclerosis: an autopsy study. *J Am Heart Assoc*. 2019;8:e013793. doi: 10.1161/JAHA.119.013793
- Numaguchi R, Furuhashi M, Matsumoto M, Sato H, Yanase Y, Kuroda Y, Harada R, Ito T, Higashiura Y, Koyama M, et al. Differential phenotypes in perivascular adipose tissue surrounding the internal thoracic artery and diseased coronary artery. *J Am Heart Assoc*. 2019;8:e011147. doi: 10.1161/JAHA.118.011147
- Harris PA, Taylor R, Thielke R, Payne J, Gonzalez N, Conde JG. Research electronic data capture (REDCap)—a metadata-driven methodology and workflow process for providing translational research informatics support. *J Biomed Inform*. 2009;42:377–381. doi: 10.1016/j.jbi.2008.08.010
- Farias-Itao DS, Pasqualucci CA, Nishizawa A, Silva LFF, Campos FM, Silva KCSD, Leite REP, Grinberg LT, Ferretti-Rebustini REL, Jacob Filho W, et al. Perivascular adipose tissue inflammation and coronary artery disease: an autopsy study protocol. *JMIR Res Protoc*. 2016;5:e211. doi: 10.2196/resprot.6340
- Suemoto CK, Ferretti-Rebustini REL, Rodriguez RD, Leite REP, Soterio L, Brucki SMD, Spera RR, Cippiciani TM, Farfel JM, Chiavegatto Filho A, et al. Neuropathological diagnoses and clinical correlates in older adults in Brazil: a cross-sectional study. *PLoS Med*. 2017;14:e1002267. doi: 10.1371/journal.pmed.1002267
- Yahagi K, Kolodgie FD, Otsuka F, Finn AV, Davis HR, Joner M, Virmani R. Pathophysiology of native coronary, vein graft, and in-stent atherosclerosis. *Nat Rev Cardiol*. 2016;13:79–98. doi: 10.1038/ncardio.2015.164
- Andrade RA, Farias-Itao DS, Nishizawa A, Campos FM, Pasqualucci CA, Suemoto CK, Campo AB. Processamento de Imagens para Análise da Composição de Placa de Aterosclerose: Estudo Preliminar em Material de Autópsia. 2017. Available at: <https://eventos.ufabc.edu.br/siimsp/files/id59.pdf>. Accessed May 16, 2021.

20. Suemoto CK, Nitrini R, Grinberg LT, Ferretti REL, Farfel JM, Leite RE, Menezes PR, Fregni F, Jacob-Filho W, Pasqualucci CA, et al. Atherosclerosis and dementia: a cross-sectional study with pathological analysis of the carotid arteries. *Stroke*. 2011;42:3614–3615. doi: 10.1161/STROKEAHA.111.628156
21. Nakatani S, Yamagishi M, Tamai J, Goto Y, Umeno T, Kawaguchi A, Yutani C, Miyatake K. Assessment of coronary artery distensibility by intravascular ultrasound: application of simultaneous measurements of luminal area and pressure. *Circulation*. 1995;91:2904–2910. doi: 10.1161/01.CIR.91.12.2904
22. Narula J, Nakano M, Virmani R, Kolodgie FD, Petersen R, Newcomb R, Malik S, Fuster V, Finn AV. Histopathologic characteristics of atherosclerotic coronary disease and implications of the findings for the invasive and noninvasive detection of vulnerable plaques. *J Am Coll Cardiol*. 2013;61:1041–1051. doi: 10.1016/j.jacc.2012.10.054
23. University of California, Los Angeles: Institute for Digital Research & Education. Regression with Stata Chapter 4—beyond OLS. Available at: <https://stats.idre.ucla.edu/stata/webbooks/reg/chapter4/regression-with-statachapter-4-beyond-ols-2/>. Accessed October 24, 2019.
24. University of California, Los Angeles: Statistical Consulting Group. How can I use countfit in choosing a count model? Available at: <https://stats.idre.ucla.edu/stata/faq/how-can-i-use-countfit-in-choosing-a-count-model/>. Accessed February 1, 2021.
25. McClain J, Hsu F, Brown E, Burke G, Carr J, Harris T, Kritchevsky S, Szklo M, Tracy R, Ding J. Pericardial adipose tissue and coronary artery calcification in the Multi-Ethnic Study of Atherosclerosis (MESA). *Obesity*. 2013;21:1056–1063. doi: 10.1002/oby.20090
26. Kroll L, Nassenstein K, Jochims M, Koitka S, Nensa F. Assessing the role of pericardial fat as a biomarker connected to coronary calcification—a deep learning based approach using fully automated body composition analysis. *J Clin Med*. 2021;10:356. doi: 10.3390/jcm10.020356
27. Colin S, Chinetti-Gbaguidi G, Staels B. Macrophage phenotypes in atherosclerosis. *Immunol Rev*. 2014;262:153–166. doi: 10.1111/immr.12218
28. Kitagawa T, Yamamoto H, Sentani K, Takahashi S, Tsumura H, Senoo A, Yasui W, Sueda T, Kihara Y. The relationship between inflammation and neoangiogenesis of epicardial adipose tissue and coronary atherosclerosis based on computed tomography analysis. *Atherosclerosis*. 2015;243:293–299. doi: 10.1016/j.atherosclerosis.2015.09.013
29. Shioi A, Ikari Y. Plaque calcification during atherosclerosis progression and regression. *J Atheroscler Thromb*. 2018;25:294–303. doi: 10.5551/jat.RV17020
30. Montanaro M, Scimeca M, Anemona L, Servadei F, Giacobbi E, Bonfiglio R, Bonanno E, Urbano N, Ippoliti A, Santeusano G, et al. The paradox effect of calcification in carotid atherosclerosis: microcalcification is correlated with plaque instability. *Int J Mol Sci*. 2021;22:395. doi: 10.3390/ijms22010395
31. Verhagen SN, Buijsrogge MP, Vink A, van Herwerden LA, van der Graaf Y, Visseren FLJ. Secretion of adipocytokines by perivascular adipose tissue near stenotic and non-stenotic coronary artery segments in patients undergoing CABG. *Atherosclerosis*. 2014;233:242–247. doi: 10.1016/j.atherosclerosis.2013.12.005
32. Konishi M, Sugiyama S, Sato Y, Oshima S, Sugamura K, Nozaki T, Ohba K, Matsubara J, Sumida H, Nagayoshi Y, et al. Pericardial fat inflammation correlates with coronary artery disease. *Atherosclerosis*. 2010;213:649–655. doi: 10.1016/j.atherosclerosis.2010.10.007
33. Margaritis M, Antonopoulos AS, Digby J, Lee R, Reilly S, Coutinho P, Shirodaria C, Sayeed R, Petrou M, De Silva R, et al. Interactions between vascular wall and perivascular adipose tissue reveal novel roles for adiponectin in the regulation of endothelial nitric oxide synthase function in human vessels. *Circulation*. 2013;127:2209–2221. doi: 10.1161/CIRCULATIONAHA.112.001133
34. Takaoka M, Suzuki H, Shioda S, Sekikawa K, Saito Y, Nagai R, Sata M. Endovascular injury induces rapid phenotypic changes in perivascular adipose tissue. *Arterioscler Thromb Vasc Biol*. 2010;30:1576–1582. doi: 10.1161/ATVBAHA.110.207175
35. McKenney-Drake ML, Rodenbeck SD, Bruning RS, Kole A, Yancey KW, Alloosh M, Sacks HS, Sturek M. Epicardial adipose tissue removal potentiates outward remodeling and arrests coronary atherogenesis. *Ann Thorac Surg*. 2017;103:1622–1630. doi: 10.1016/j.athoracsur.2016.11.034
36. Kanaji Y, Hirano H, Sugiyama T, Hoshino M, Horie T, Misawa T, Nogami K, Ueno H, Hada M, Yamaguchi M, et al. Pre-percutaneous coronary intervention pericoronary adipose tissue attenuation evaluated by computed tomography predicts global coronary flow reserve after urgent revascularization in patients with non-ST-segment-elevation acute coronary syndrome. *J Am Heart Assoc*. 2020;9:e016504. doi: 10.1161/JAHA.120.016504
37. Hedgire S, Baliyan V, Zucker EJ, Bittner DO, Staziaki PV, Takx RAP, Scholtz J-E, Meyersohn N, Hoffmann U, Ghoshhajra B. Perivascular epicardial fat stranding at coronary CT angiography: a marker of acute plaque rupture and spontaneous coronary artery dissection. *Radiology*. 2018;287:808–815. doi: 10.1148/radiol.2017171568
38. Oikonomou EK, Marwan M, Desai MY, Mancio J, Alashi A, Hutt Centeno E, Thomas S, Herdman L, Kotanidis CP, Thomas KE, et al. Non-invasive detection of coronary inflammation using computed tomography and prediction of residual cardiovascular risk (the CRISP CT study): a post-hoc analysis of prospective outcome data. *Lancet*. 2018;392:929–939. doi: 10.1016/S0140-6736(18)31114-0
39. Cho KY, Miyoshi H, Kuroda S, Yasuda H, Kamiyama K, Nakagawara J, Takigami M, Kondo T, Atsumi T. The phenotype of infiltrating macrophages influences arteriosclerotic plaque vulnerability in the carotid artery. *J Stroke Cerebrovasc Dis*. 2013;22:910–918. doi: 10.1016/j.jstrokecerebrovasdis.2012.11.020
40. Tanaka K, Nagata D, Hirata Y, Tabata Y, Nagai R, Sata M. Augmented angiogenesis in adventitia promotes growth of atherosclerotic plaque in apolipoprotein E-deficient mice. *Atherosclerosis*. 2011;215:366–373. doi: 10.1016/j.atherosclerosis.2011.01.016
41. Ito H, Wakatsuki T, Yamaguchi K, Fukuda D, Kawabata Y, Matsuura T, Kusunose K, Ise T, Tobiume T, Yagi S, et al. Atherosclerotic coronary plaque is associated with adventitial vasa vasorum and local inflammation in adjacent epicardial adipose tissue in fresh cadavers. *Circ J*. 2020;84:769–775. doi: 10.1253/circj.CJ-19-0914
42. Ohyama K, Matsumoto Y, Takanami K, Ota H, Nishimiya K, Sugisawa J, Tsuchiya S, Amamizu H, Uzuka H, Suda A, et al. Coronary adventitial and perivascular adipose tissue inflammation in patients with vasospastic angina. *J Am Coll Cardiol*. 2018;71:414–425. doi: 10.1016/j.jacc.2017.11.046
43. Khallou-Laschet J, Varthaman A, Fornasa G, Compain C, Gaston A, T, Clement M, Dussiot M, Levillain O, Raff-Dubois S, Nicoletti A, et al. Macrophage plasticity in experimental atherosclerosis. *PLoS One*. 2010;5:e8852. doi: 10.1371/journal.pone.0008852
44. Lumeng CN, Bodzin JL, Saltiel AR. Obesity induces a phenotypic switch in adipose tissue macrophage polarization. *J Clin Invest*. 2007;117:175–184. doi: 10.1172/JCI29881
45. Ferretti REDL, Damin AE, Brucki SMD, Morillo LS, Perroco TR, Campora F, Moreira EG, Balbino ES, Lima MDCDA, Battela C, et al. Post-Mortem diagnosis of dementia by informant interview. *Dement Neuropsychol*. 2010;4:138–144. doi: 10.1590/S1980-57642010DN40200011
46. Farfel JM, Nitrini R, Suemoto CK, Grinberg LT, Ferretti REL, Leite REP, Tampellini E, Lima L, Farias DS, Neves RC, et al. Very low levels of education and cognitive reserve: a clinicopathologic study. *Neurology*. 2013;81:650–657. doi: 10.1212/WNL.0b013e3182a08f1b
47. Fernández-Friera L, Fuster V, López-Melgar B, Oliva B, Sánchez-González J, Macías A, Pérez-Asenjo B, Zamudio D, Alonso-Farto JC, España S, et al. Vascular inflammation in subclinical atherosclerosis detected by hybrid PET/MRI. *J Am Coll Cardiol*. 2019;73:1371–1382. doi: 10.1016/j.jacc.2018.12.075
48. Emini Veseli B, Perrotta P, De Meyer GRA, Roth L, Van der Donck C, Martinet W, De Meyer GRY. Animal models of atherosclerosis. *Eur J Pharmacol*. 2017;816:3–13. doi: 10.1016/j.ejphar.2017.05.010
49. Ridker PM, Everett BM, Thuren T, MacFadyen JG, Chang WH, Ballantyne C, Fonseca F, Nicolau J, Koenig W, Anker SD, et al. Antiinflammatory therapy with canakinumab for atherosclerotic disease. *N Engl J Med*. 2017;377:1119–1131. doi: 10.1056/NEJMoa1707914
50. Tardif J-C, Kouz S, Waters DD, Bertrand OF, Diaz R, Maggioni AP, Pinto FJ, Ibrahim R, Gamra H, Kivan GS, et al. Efficacy and safety of low-dose colchicine after myocardial infarction. *N Engl J Med*. 2019;381:2497–2505. doi: 10.1056/NEJMoa1912388

## SUPPLEMENTARY MATERIAL

### **Macrophage polarization in the perivascular fat was associated with coronary atherosclerosis**

**Short title: Macrophage inflammation and atherosclerosis**

**Authors:**

Daniela Souza Farias-Itao, BSN MSc;<sup>1</sup> Carlos Augusto Pasqualucci, MD PhD;<sup>1</sup> Renato Araújo de Andrade BE PSM;<sup>2</sup> Luiz Fernando Ferraz da Silva, MD PhD;<sup>1</sup> Maristella Yahagi-Estevam, BPT;<sup>1</sup> Silvia Helena Gelas Lage, MD PhD,<sup>3</sup> Renata Elaine Paraízo Leite, BPT PhD;<sup>1</sup>Alexandre Brincalpe Campo, BE PhD;<sup>2</sup> Claudia Kimie Suemoto, MD MSc PhD<sup>1,4</sup>

**Affiliations:**

<sup>1</sup> Department of Pathology, University of Sao Paulo Medical School, Sao Paulo, Brazil;

<sup>2</sup> Control and Automation Engineering, Federal Institute of Education, Science and Technology of Sao Paulo, Sao Paulo, Brazil;

<sup>3</sup> Heart Institute (InCor), University of Sao Paulo Medical School, Sao Paulo, Brazil;

<sup>4</sup> Discipline of Geriatrics, University of Sao Paulo Medical School, Sao Paulo, Brazil.

***Materials & Correspondence***

Daniela Souza Farias-Itao BSN MSc  
Faculdade de Medicina da Universidade de São Paulo  
455 Avenida Doutor Arnaldo, sala 1355  
01246-903  
São Paulo, SP, Brazil,  
Phone and Fax: +55-11-3061-8249  
E-mail: dsfarias@usp.br

## SUPPLEMENTARY METHODS

### Hematoxylin-eosin stain technique

The slides were stained with hematoxylin-eosin, as per the following steps: deparaffinization and hydration of the slides; after, stained with Harris's hematoxylin for five minutes; and washed under running water. The slides were differentiated in acid-alcohol; turned blue with ammoniacal acid; washed under running water; bathed in 95% of ethanol diluted in deionized water; bathed in eosin for two minutes; washed under running water, dehydrated, diaphanized, and mounted on slides. We prepared the hematoxylin-eosin by dissolving in alcohol and dissolving the alum in the water, heating it without boiling. It was then removed from heat and the two solutions were mixed. It was brought to the boil quickly, always stirring with a glass stick (time should not exceed 1 minute). After that, it was removed from the heat and cooled under running water (thermal shock). The next day, the solution was heated again and the mercury oxide added. It was then cooled quickly, under running water.

#### *1% Eosin stock solution:*

Yellow Eosin Y: ..... 1 g

Distilled water: ..... 100 mL

#### *1% Phloxine stock solution*

Phloxine B: ..... 1g

Distilled water: ..... 100 ml

#### *Eosin-Phloxine Solution*

1% Eosin stock solution: ..... 100 mL

1% Phloxine stock solution: ..... 10mL

96% Alcohol: ..... 780 mL

Glacial acetic acid: ..... 5 mL

### Masson's trichrome stain technique

The slides were stained with *Masson's trichrome* according to the steps: the slides were deparaffinized and hydrated; stained with Weigert's iron hematoxylin for ten minutes, washed in current water for ten minutes, and bathed with deionized water. Next, we stained with Scarlet Biebrich solution for one minute, washed under running water, and bathed with deionized water. We then, differentiated with Phosphotungstic-Phosphomolybdic Acid solution for 10 to 15 minutes, stained with aniline blue for 10 to 15 minutes, followed by bathing in deionized water, dehydration, and diaphanization, and finally, the slides were mounted in resin.

### *Weigert's Ferric Hematoxylin*

#### *Solution A*

Hematoxylin powder ..... 1 g  
95% Alcohol ..... 100mL

#### *Solution B*

Aqueous 30% Ferric Chloride solution ..... 4 mL  
Distilled water..... 95 mL  
Concentrated Hydrochloric Acid ..... 1 mL

Working solution: combine equal parts of solutions A and B at the time of use.

### *Biebrich's Scarlet Solution*

Aqueous solution of Scarlet Biebrich 1% ..... 90 mL.  
Aqueous solution of Acid Fuchsin 1% ..... 10 mL  
Glacial Acetic Acid 1% ..... 1mL

### *Phosphotungstic-Phosphomolybdic Acid Solution*

Phosphotungstic Acid ..... 2.5 g

Phosphomolybdic acid ..... 2.5 g  
Distilled water ..... 100 mL

*Aniline Blue Solution*

Aniline Blue ..... 2.5 g  
Glacial Acetic Acid ..... 2mL  
Distilled water ..... 100 mL

Boil the water, then dissolve the blue and filter; add the acid last.

*Verhoeff stain technique*

The slides were stained with Verhoeff according to the following steps: the slides were deparaffinized and hydrated; bathing in Bouin for one minute and washing until the yellow color came out. Then, we stained with hematoxylin-eosin for 25 minutes, washed under running water, differentiated in 2% Ferric Chloride until the elastic fibers were clearly visualized, washed under running water for five minutes, bathed in 96% alcohol for five minutes, and washed under running water for five minutes. Next, we stained with Van-Gieson dye for one minute, washed, dehydrated, and mounted on slides.

*Bouin*

Picric Acid ..... 800 mL  
Pure formaldehyde ..... 200 mL

*Alcoholic Hematoxylin 5% ..... 30 mL*

Hematoxylin ..... 5 g  
Absolute alcohol ..... 100mL

*10% Ferric Chloride ..... 12mL*



Ferric Chloride ..... 10 g  
Distilled water ..... 100 mL

*Lugol - 12 ml*

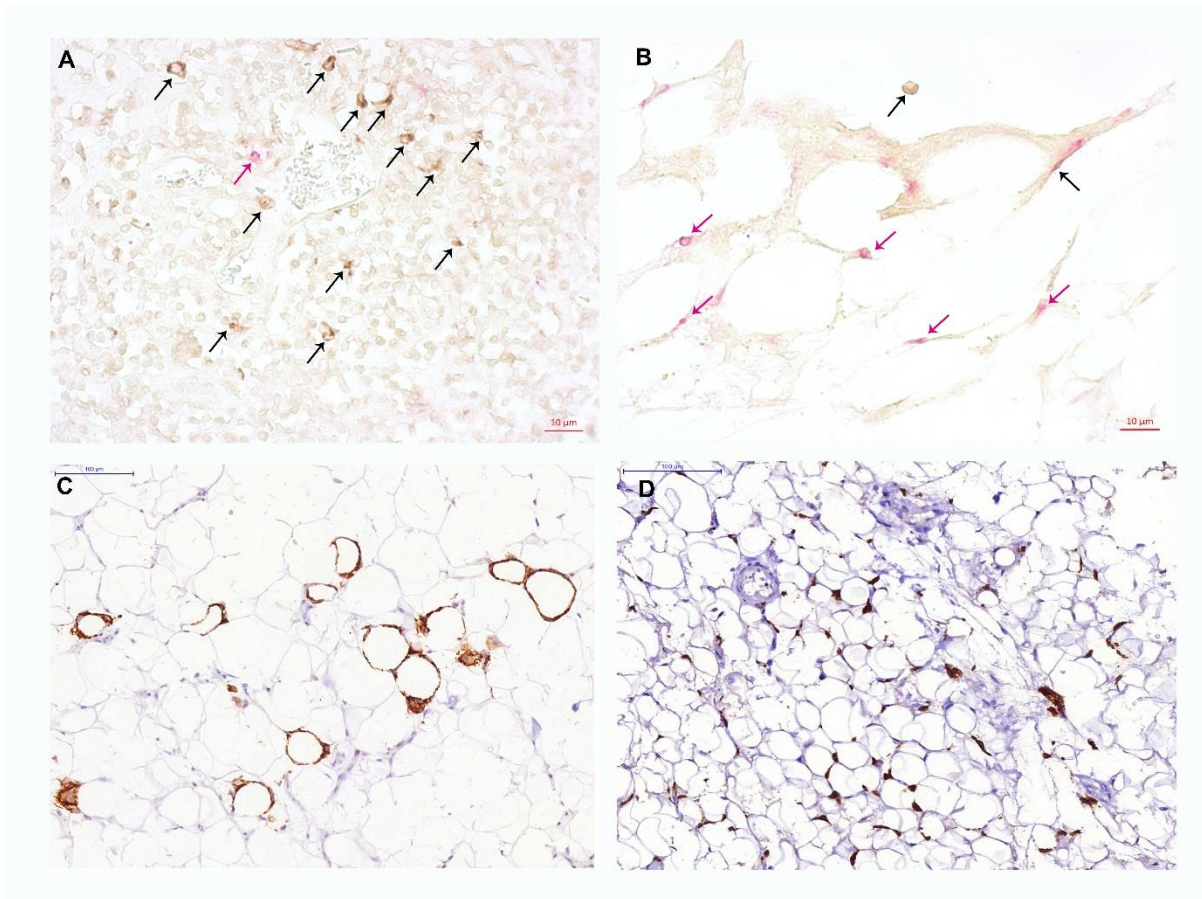
Potassium iodide ..... 4 g  
Iodine..... 2 g  
Distilled water ..... 100mL

Dissolve the Potassium Iodide and then the iodine, together with the water.

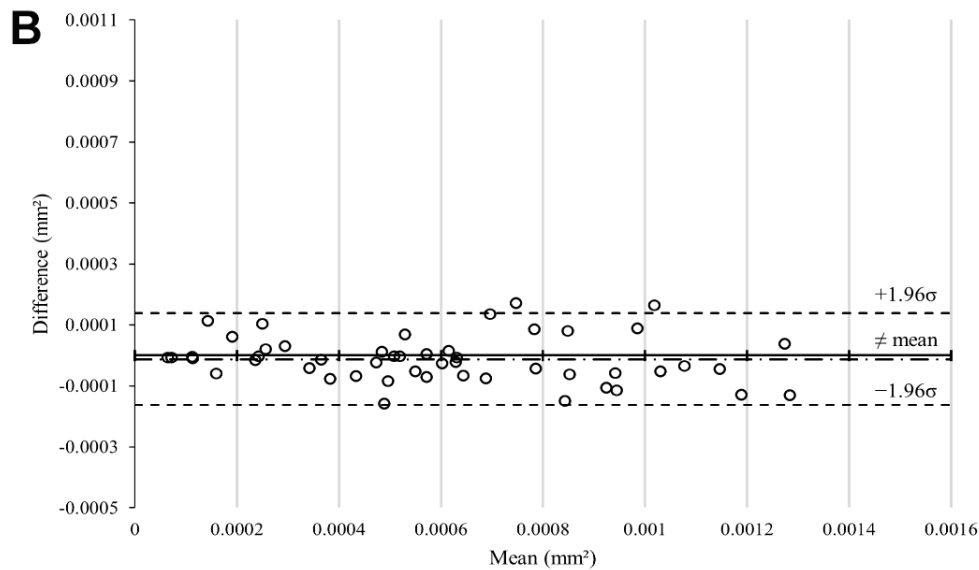
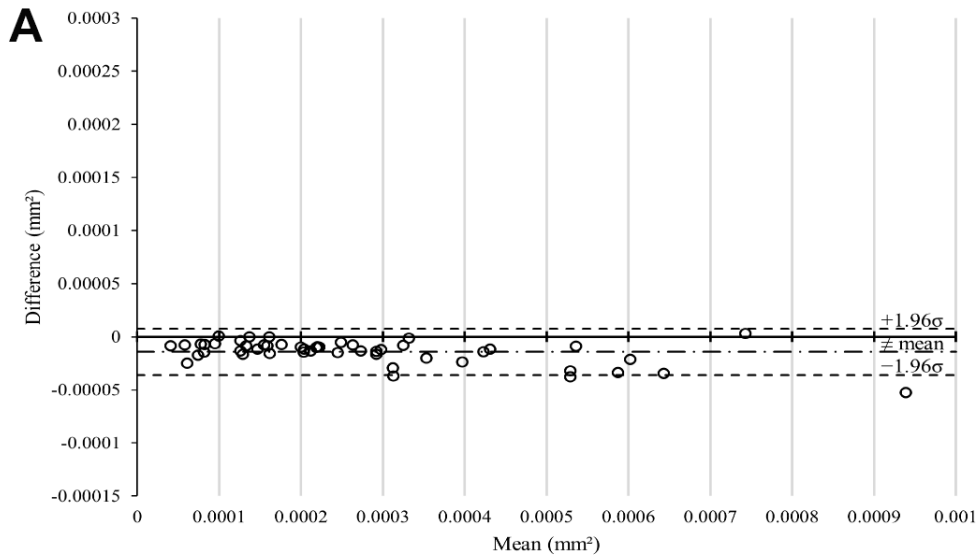
*Van-Gieson*

Saturated aqueous solution of picric acid ..... 97.5 mL  
Acid fuchsin 1% aqueous solution ..... 2.5 mL

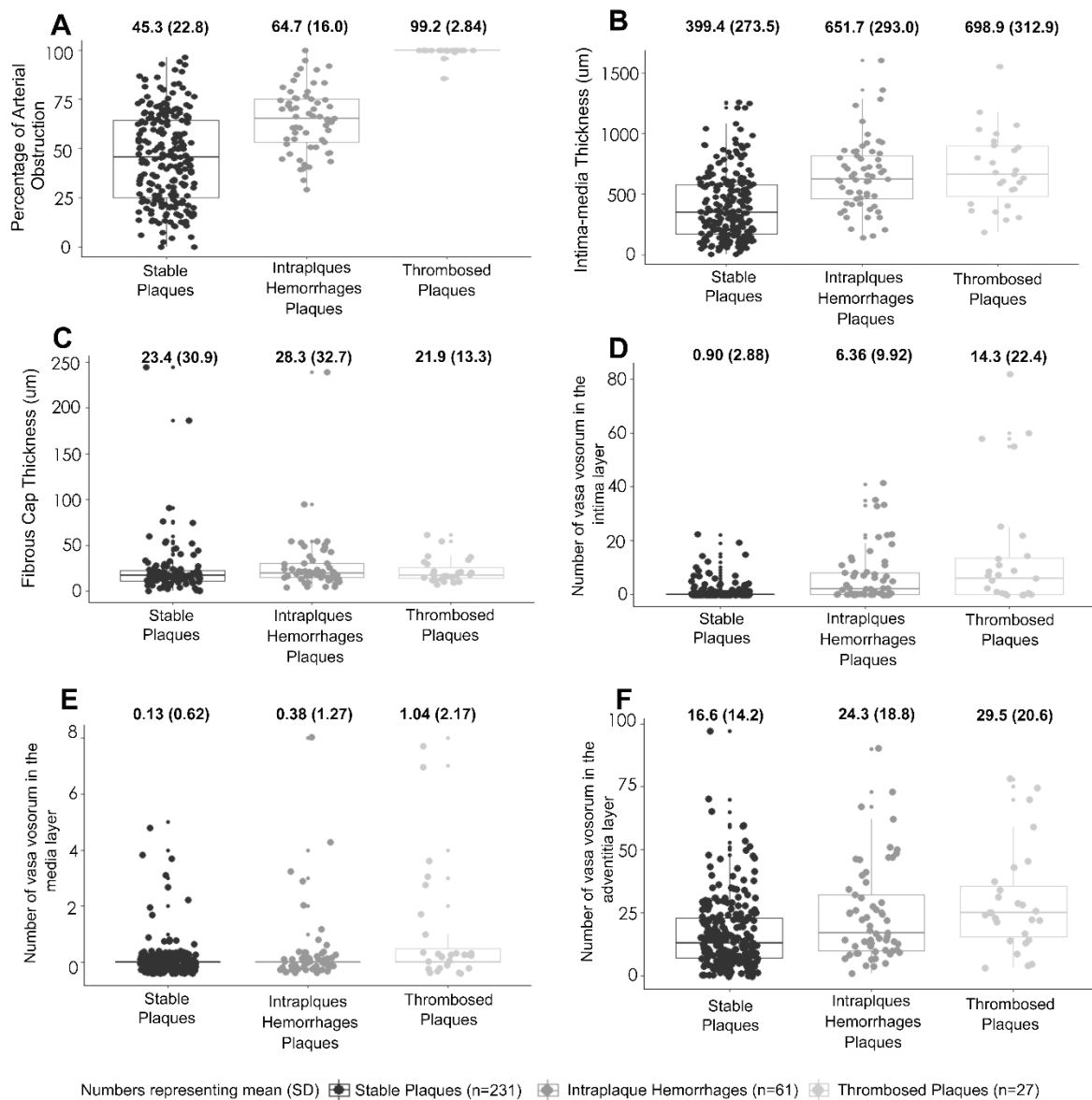
## SUPPLEMENTARY FIGURES



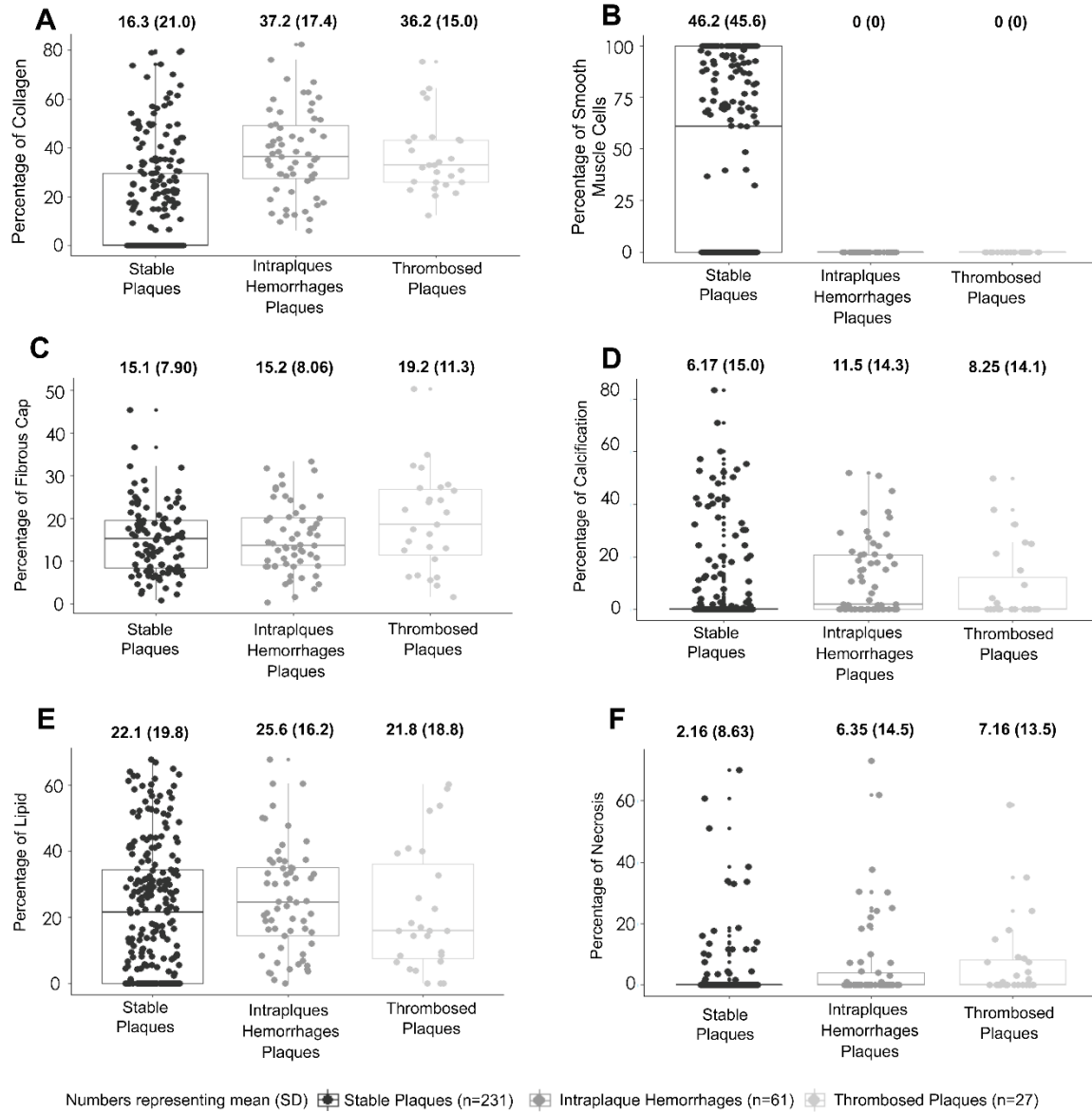
Supplementary Figure I. Polarized macrophages in the periadipose pericoronary adipose tissue. A: Pharyngeal tonsil double-stained using immunohistochemistry technique with M1 macrophages CD11c<sup>+</sup> (black arrows) and M2 macrophages CD206<sup>+</sup> (pink arrows); B: Perivascular adipose tissue adjacent to coronary artery with atherosclerotic plaque double-stained using immunohistochemistry technique with M1 macrophages CD11c<sup>+</sup> (black arrows) and M2 macrophages CD206<sup>+</sup> (pink arrows); C: Perivascular adipose tissue adjacent to the coronary artery with atherosclerotic plaque using immunohistochemistry with M1 macrophages (brown immunostaining). Macrophages M1 forming a crown-like structures around the adipocyte in death or death process.



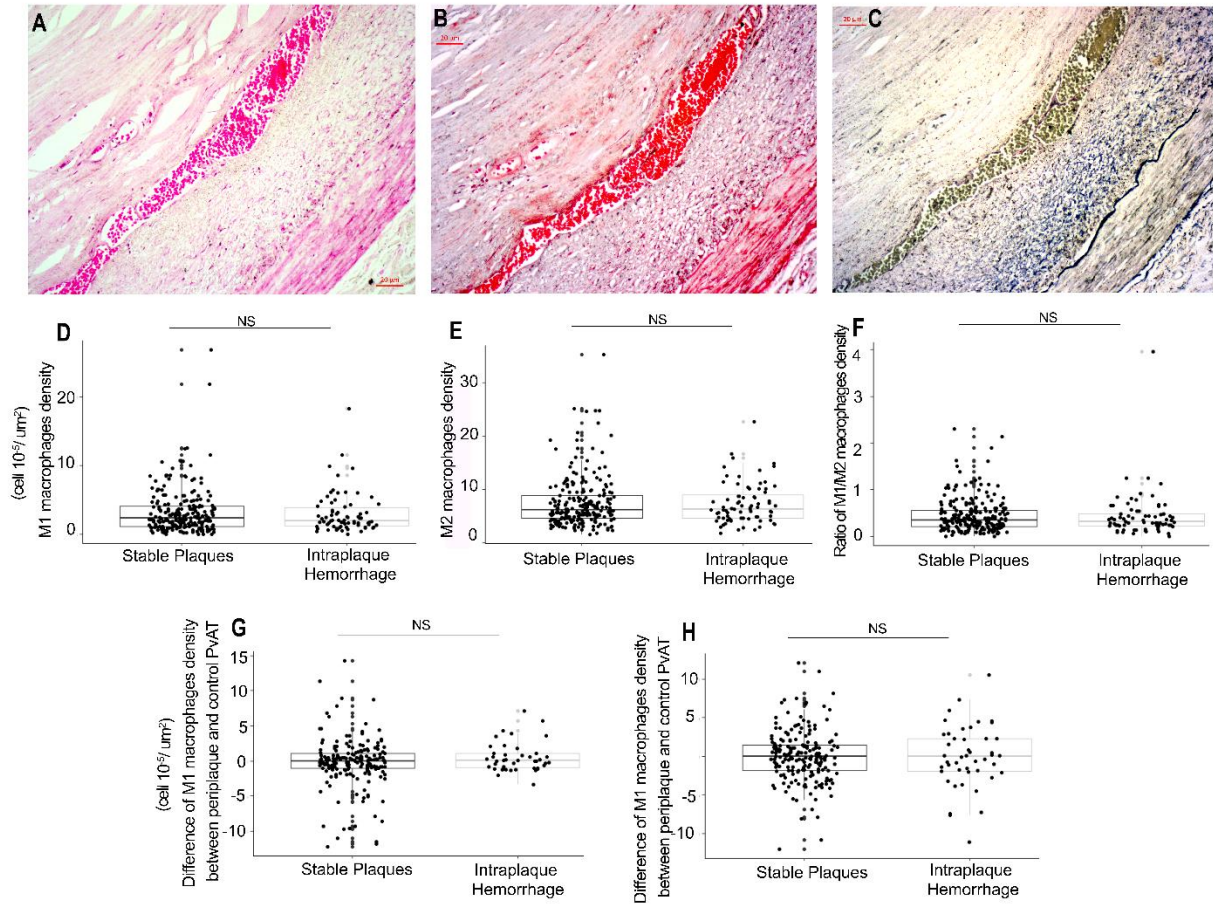
Supplementary Figure II. Agreement of lumen and internal elastic lamina measurements made by artificial intelligence and expertise in the APA software (n=50 arterial segments). A: Bland-Altman graph showing the difference between the contour of lumen when executed by the APA software and when measured manually by a human expert. The circles inside the interval  $+1.96\sigma$  to  $-1.96\sigma$  correspond to 94% agreement. B: Bland-Altman graph showing the difference between the contour of internal elastic lamina measured by the APA software and manually by a human expert. The circles inside the interval  $+1.96\sigma$  to  $-1.96\sigma$  correspond to 94% agreement.



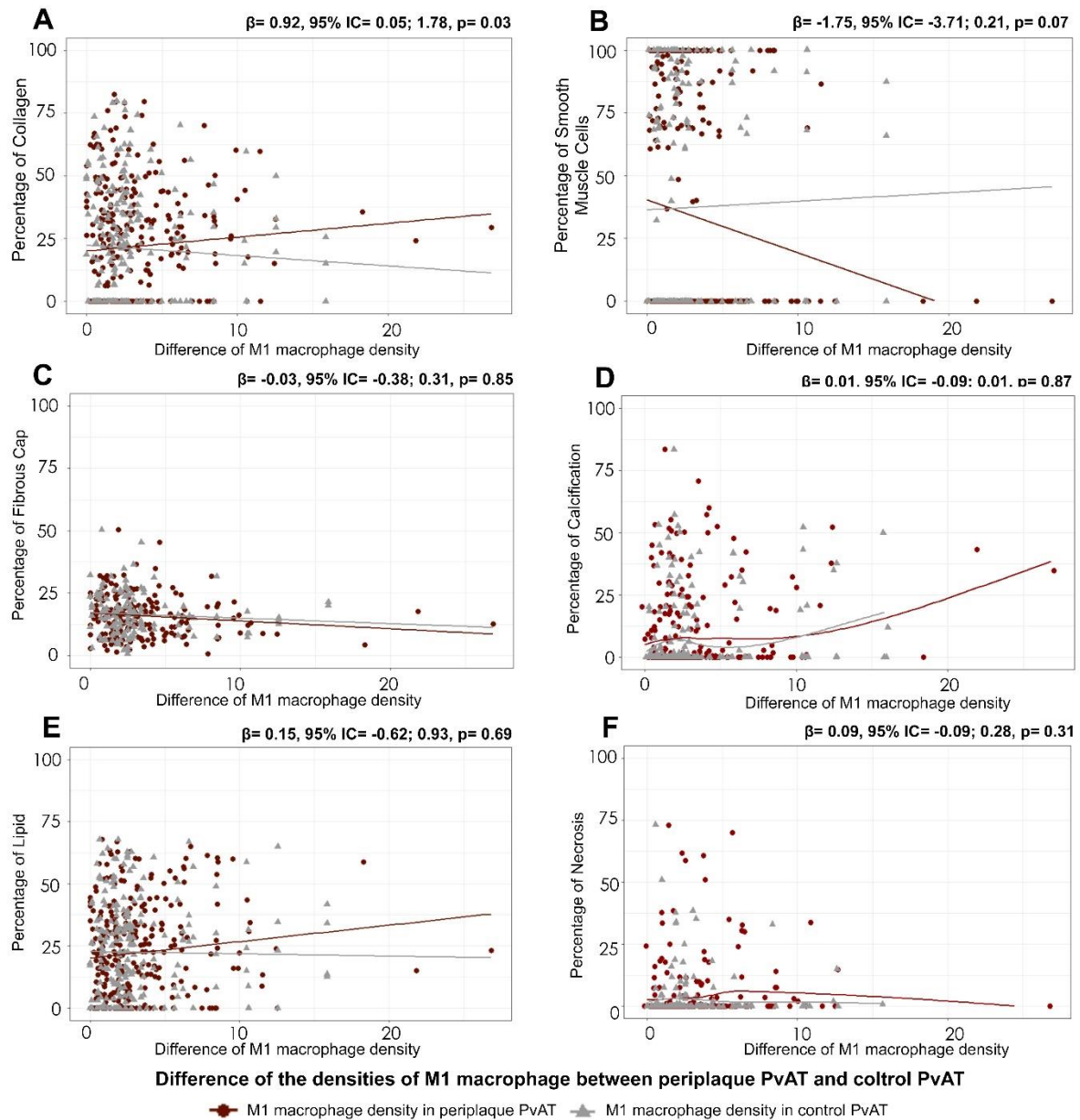
Supplementary Figure III. Boxplot with jitter plot of atherosclerotic plaque measurements in coronary arteries by plaque classification (n=319 arterial segments). A: Boxplot with jitter plot of percentage of arterial obstruction by plaque classification; B: Boxplot with jitter plot of intima-media thickness by plaque classification; C: Boxplot with jitter plot of fibrous cap thickness by plaque classification; D: Boxplot with jitter plot of the number of *vasa vasorum* in the intima layer by plaque classification; E: Boxplot with jitter plot of the number of *vasa vasorum* in the media layer by plaque classification; F: Boxplot with jitter plot of the number of *vasa vasorum* in the adventitia layer by plaque classification.



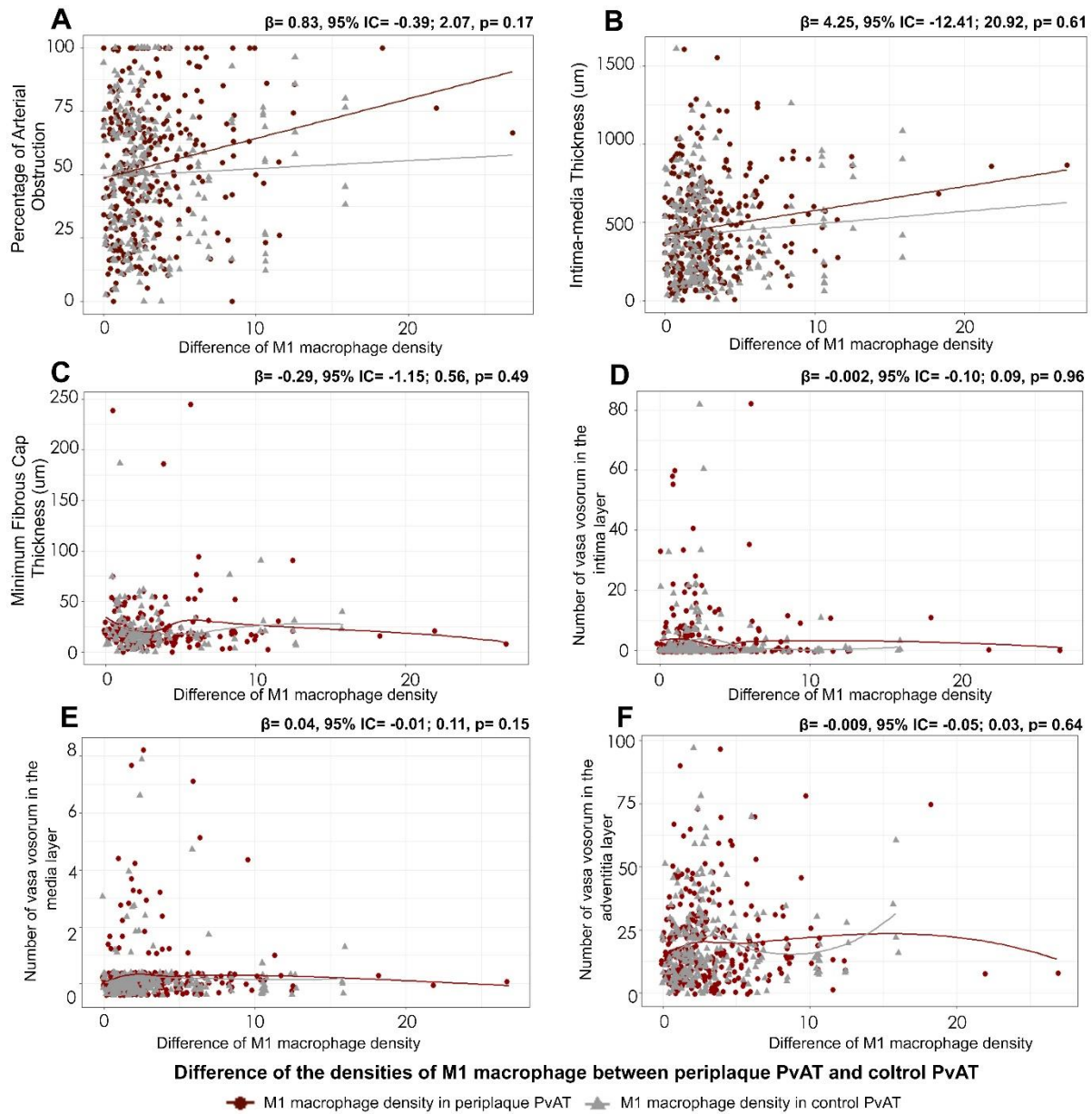
Supplementary Figure IV. Boxplot with jitter plot of atherosclerotic plaque components in coronary arteries by plaque classification (n=319 arterial segments). A: Boxplot with jitter plot of percentage of collagen content in atherosclerotic plaques by plaque classification; B: Boxplot with jitter plot of percentage of smooth muscle cell content in atherosclerotic plaques by plaque classification; C: Boxplot with jitter plot of percentage of fibrous cap content in atherosclerotic plaques by plaque classification; D: Boxplot with jitter plot of percentage of calcification content in atherosclerotic plaques by plaque classification; E: Boxplot with jitter plot of percentage of lipid content in atherosclerotic plaques by plaque classification; F: Boxplot with jitter plot of percentage of necrosis in atherosclerotic plaques by plaque classification.



Supplementary Figure V. Association between the polarized macrophages density in the perivascular adipose tissue and intraplaque hemorrhage (n=319 arterial segments). A: Atherosclerotic plaque with the presence of intraplaque hemorrhage, hematoxylin-eosin stain; B: Atherosclerotic plaque with the presence of intraplaque hemorrhage, Masson's Trichrome stain; C: Atherosclerotic plaque with the presence of intraplaque hemorrhage, Verhoeff stain; D-H: Association between the polarized macrophages density in the PvAT and atherosclerotic plaques with intraplaque hemorrhage (n=319 arterial segments). NS: non-significant.

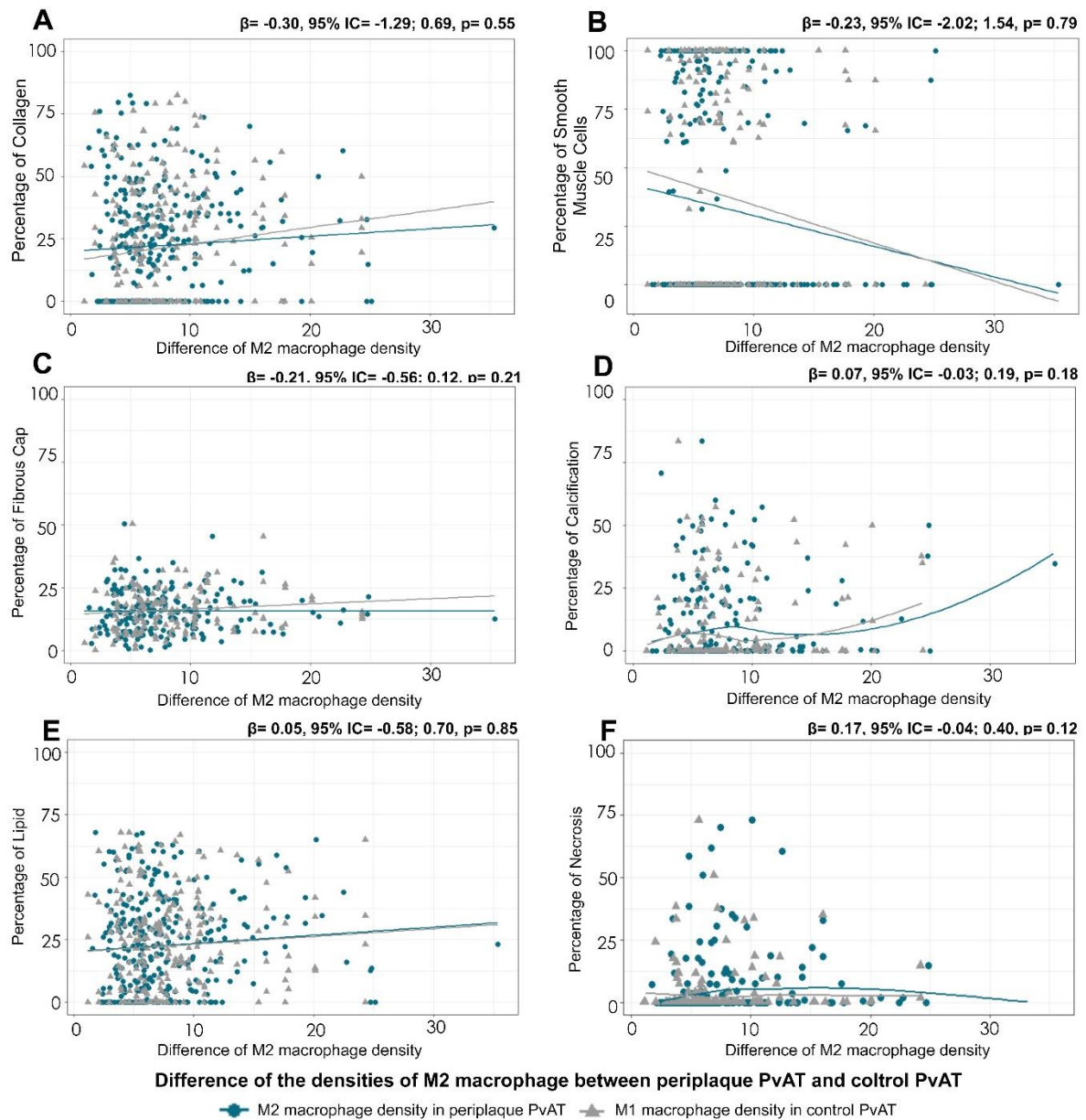


Supplementary Figure VI. Association of the difference of M1 macrophage density in the periplaque PvAT and control PvAT with the measures of atherosclerotic plaque components in coronary arteries (n=319 coronary arteries). A, B, C, and E: Linear regression adjusted for repeated measures in the same individual and confounding factors (i.e. age, sex, hypertension, diabetes, body mass index, physical inactivity, alcohol consumption, and smoking); D and F: Negative binomial adjusted for repeated measures in the same individual and confounding factors.

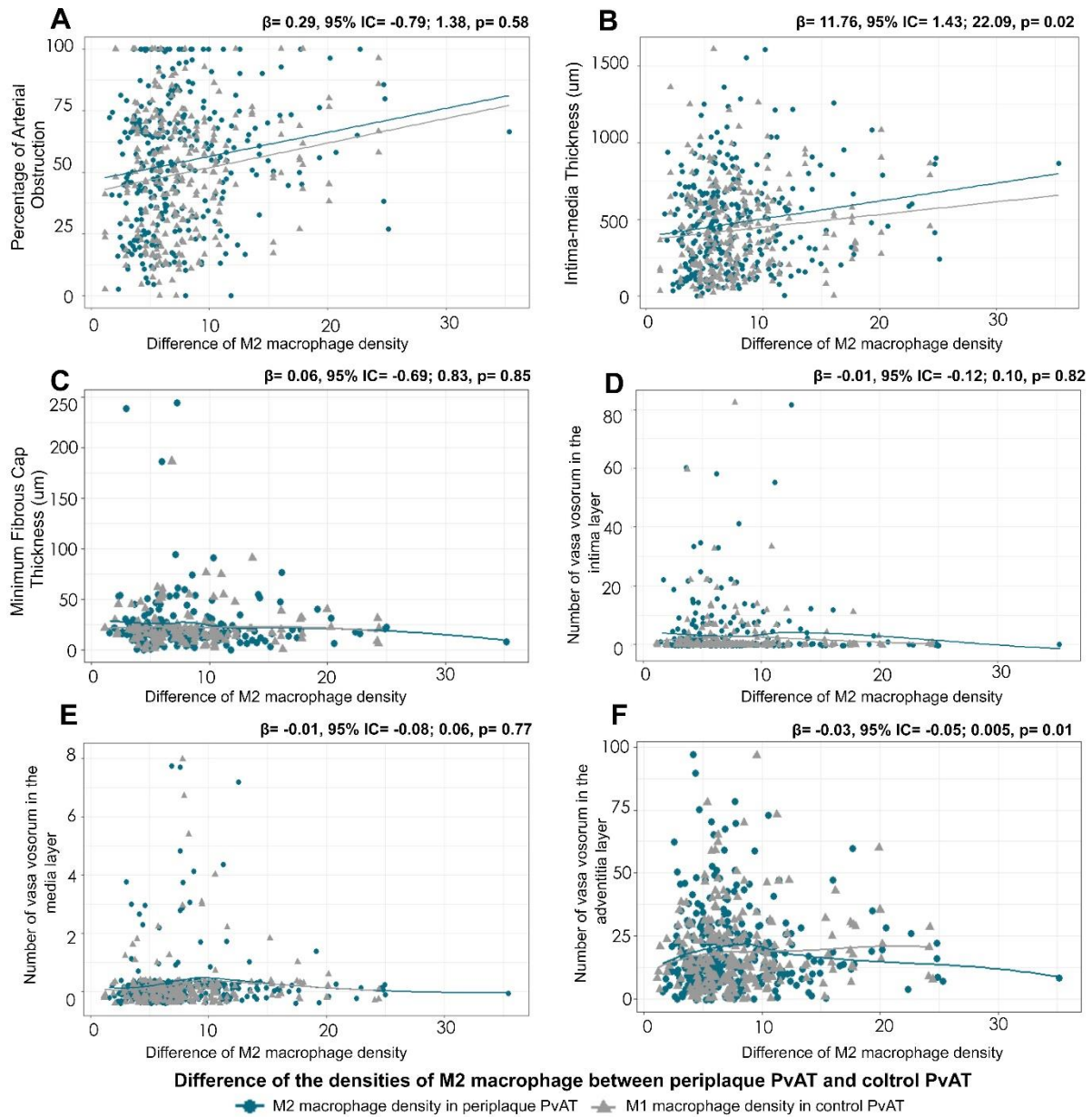


Supplementary Figure VII. Association of the difference of M1 macrophage density in the periplaque PvAT and control PvAT with the measures of atherosclerotic plaque in coronary arteries (n=319 coronary arteries). A and B: Linear regression adjusted for repeated measures in the same individual and confounding factors (i.e. age, sex, hypertension, diabetes, body mass index, physical inactivity, alcohol consumption, and smoking); C: Negative binomial regression adjusted for repeated measures in the same individual and confounding factors. D, E and F: Poisson regression adjusted for repeated measures in the same individual and confounding factors.





Supplementary Figure VIII. Association of the difference of M2 macrophage density in the periplaque PvAT and control PvAT with the measures of atherosclerotic plaque components in coronary arteries (n=319 coronary arteries). A, B, C and E: Correlation using linear regression adjusted for repeated measures in the same individual and confounding factors (i.e. age, sex, hypertension, diabetes, body mass index, physical inactivity, alcohol consumption, and smoking); D and F: Correlation using negative binomial adjusted for repeated measures in the same individual and confounding factors.



Supplementary Figure IX. Association of the difference of M2 macrophage density in the periplaque PvAT and control PvAT with the measures of atherosclerotic plaque in coronary arteries (n=319 coronary arteries). A and B: Correlation using linear regression adjusted for repeated measures in the same individual and confounding factors (i.e. age, sex, hypertension, diabetes, body mass index, physical inactivity, alcohol consumption, and smoking); C: Correlation using negative binomial regression adjusted for repeated measures in the same individual and confounding factors. D, E and F: Correlation using Poisson regression adjusted for repeated measures in the same individual and confounding factors.

## SUPPLEMENTARY TABLES

Supplementary Table I. Characterization of the sample (n=82 subjects).

Variable	Mean (SD) or n (%)
<b>Age (years)</b>	69.0 (14.4)
<b>Female</b>	41 (50%)
<b>Race</b>	
<i>White</i>	48 (58%)
<i>Black and Asian</i>	34 (42%)
<b>Education (years), median (IQR)</b>	4 (1-6)
<b>Hypertension</b>	61 (74%)
<b>Diabetes</b>	30 (36%)
<b>CAD symptoms</b>	10 (12%)
<b>Heart failure</b>	19 (23%)
<b>Stroke</b>	10 (12%)
<b>Dyslipidemia</b>	14 (17%)
<b>BMI (kg/m<sup>2</sup>)</b>	24.4 (5.8)
<b>Physical inactivity</b>	56 (68%)
<b>Current smoking</b>	12 (15%)
<b>Current alcohol use</b>	24 (29%)
<i>Antihypertensive drugs</i>	45 (55%)
<i>Hypoglycemic drugs</i>	24 (29%)
<i>Insulin</i>	7 (8%)
<i>Lipid-lowering drugs</i>	6 (7%)
<b>Density of M1 CD11c<sup>+</sup>macrophages periplaque PvAT (cell 10<sup>5</sup>/um<sup>2</sup>)*</b>	3.18 (3.17)
<b>Density of M2 CD206<sup>+</sup>macrophages periplaque PvAT (cell 10<sup>5</sup>/um<sup>2</sup>) †</b>	7.55 (4.57)
<b>Ratio of the densities between M1 CD11c<sup>+</sup>/M2 CD206<sup>+</sup> periplaque PvAT ‡</b>	0.44 (0.40)
<b>Difference of M1 CD11c<sup>+</sup> between periplaque and control PvAT §</b>	-0.10 (3.34)
<b>Difference of M2 206<sup>+</sup> between periplaque and control PvAT   </b>	0.02 (3.48)

SD: standard deviation; IQR: interquartile interval; CAD: coronary artery disease; BMI: body mass index.

\* Number of periplaque PvAT quantified for M1 CD11c<sup>+</sup>macrophages: 305.

† Number of periplaque PvAT quantified for M2 CD11c<sup>+</sup>macrophages: 308.

‡ Number of periplaque PvAT calculated for the ratio M1 CD11c<sup>+</sup>/M2 CD206<sup>+</sup> macrophages: 299.

§ Number of subtractions of M1 CD11c<sup>+</sup> between periplaque and control PvAT: 228.

|| Number of subtractions of M2 CD206<sup>+</sup> between periplaque and control PvAT: 240.

Supplementary Table II. Correlation of the M2 CD206<sup>+</sup> macrophage density of in the peri-plaque PvAT with coronary artery atherosclerosis (n=319 arterial segments).

<b>M2 CD206<sup>+</sup> macrophages density (cell 10<sup>-5</sup>/um<sup>2</sup>)</b>	<b>Unadjusted Model</b>			<b>Adjusted Model*</b>		
	<b>Coef.</b>	<b>95% CI</b>	<b>p</b>	<b>Coef.</b>	<b>95% CI</b>	<b>p</b>
<b><i>Arterial Obstruction, (%) †</i></b>	0.97	0.33; 1.61	0.003	0.77	0.12; 1.42	0.02
<b><i>IMT, μm †</i></b>	11.62	4.57; 18.68	0.002	9.09	1.54; 16.63	0.01
<b><i>Collagen, (%) †</i></b>	0.30	-0.38; 0.98	0.38	0.05	-0.59; 0.70	0.87
<b><i>Smooth Muscle Cell, (%) †</i></b>	-1.30	-2.64; 0.02	0.05	-0.74	-1.93; 0.43	0.21
<b><i>Fibrous Cap, (%) †</i></b>	-0.001	-0.24; 0.23	0.99	0.02	-0.25; 0.30	0.86
<b><i>Minimum FCT, μm ‡</i></b>	-0.38	-0.96; 0.20	0.19	-0.41	-1.08; 0.24	0.21
<b><i>Calcification, (%) ‡</i></b>	0.02	-0.01; 0.06	0.18	0.09	0.01; 0.18	0.03
<b><i>Lipid, (%) †</i></b>	0.32	-0.10; 0.76	0.14	0.15	-0.30; 0.60	0.50
<b><i>Necrosis, (%) ‡</i></b>	0.07	-0.03; 0.17	0.18	0.06	-0.06; 0.19	0.31
<b><i>Intraplaque Hemorrhage, (%) ‡</i></b>	0.03	-0.07; 0.13	0.55	0.05	-0.07; 0.18	0.40
<b><i>Vasa vasorum intima layer, n §</i></b>	-0.02	-0.10; 0.04	0.50	-0.04	-0.11; 0.02	0.23
<b><i>Vasa Vasorum media layer, n §</i></b>	0.01	-0.04; 0.06	0.68	-0.03	-0.10; 0.04	0.40
<b><i>Vasa vasorum adventitia layer, n §</i></b>	-0.003	-0.02; 0.01	0.72	-0.007	-0.02; 0.01	0.49

Coef.: Coefficient; CI: confidence level; IMT: Intima-media thickness; FCT: fibrous cap thickness.

\* Adjusted for age, sex, hypertension, diabetes, body mass index, physical inactivity, alcohol consumption, and smoking.

† Linear regression with standard error adjusted for repeated measures in the same individual.

‡ Negative binomial regression with standard error adjusted for repeated measures in the same individual.

§ Poisson regression with standard error adjusted for repeated measures in the same individual.

Supplementary Table III. Association of the polarized macrophage density in the PvAT with unstable atherosclerotic plaques (n=319 arterial segments).

Unstable Plaques	<u>Unadjusted Model</u>			<u>Adjusted Model</u>		
	OR	95% CI	p†	OR	95% CI	p‡
<b>Periplaque PvAT (cell 10<sup>-5</sup>/um<sup>2</sup>)</b>						
<b><i>Thrombosis</i></b>						
. Macrophages M1 CD11c <sup>+</sup>	1.10	1.01; 1.20	0.02	1.11	1.01; 1.23	0.03
. Macrophages M2 CD206 <sup>+</sup>	1.04	0.98; 1.10	0.15	1.04	0.97; 1.11	0.22
. Ratio M1 CD11c <sup>+</sup> /M2 CD206 <sup>+</sup>	1.92	0.97; 3.82	0.06	1.95	1.05; 3.61	0.03
<b><i>Intraplaque Hemorrhage</i></b>						
. Macrophages M1 CD11c <sup>+</sup>	0.97	0.87; 1.07	0.60	0.95	0.85; 1.07	0.45
. Macrophages M2 CD206 <sup>+</sup>	0.98	0.91; 1.07	0.80	0.97	0.90; 1.06	0.64
. Ratio M1 CD11c <sup>+</sup> /M2 CD206 <sup>+</sup>	0.98	0.40; 2.36	0.97	0.96	0.41; 2.22	0.92
<b>Difference of PvAT periplaque and control (cell 10<sup>-5</sup>/um<sup>2</sup>)</b>						
<b><i>Thrombosis</i></b>						
. Macrophages M1 CD11c <sup>+</sup>	1.22	1.03; 1.44	0.01	1.19	0.98; 1.45	0.07
. Macrophages M2 CD206 <sup>+</sup>	1.12	0.91; 1.37	0.25	1.06	0.86; 1.31	0.53
<b><i>Intraplaque Hemorrhage</i></b>						
. Macrophages M1 CD11c <sup>+</sup>	1.06	0.98; 1.15	0.09	1.05	0.97; 1.14	0.21
. Macrophages M2 CD206 <sup>+</sup>	0.99	0.86; 1.14	0.93	0.97	0.84; 1.12	0.75

OR: Odds Ratio; CI: Confidence Interval; PvAT: perivascular adipose tissue.

† Logistic regression with standard error adjusted for repeated measures in the same individual.

‡ Logistic regression with standard error adjusted for repeated measures in the same individual adjusted for age, sex, BMI, hypertension, diabetes, physical activity, alcohol consumption, and smoking.

### Major Resources Table

In order to allow validation and replication of experiments, all essential research materials listed in the Methods should be included in the Major Resources Table below. Authors are encouraged to use public repositories for protocols, data, code, and other materials and provide persistent identifiers and/or links to repositories when available. Authors may add or delete rows as needed.

#### Animals (in vivo studies)

Species	Vendor or Source	Background Strain	Sex	Persistent ID / URL

#### Genetically Modified Animals

	Species	Vendor or Source	Background Strain	Other Information	Persistent ID / URL
Parent - Male					
Parent - Female					

#### Antibodies

Target antigen	Vendor or Source	Catalog #	Working concentration	Lot # (preferred but not required)	Persistent ID / URL
Anti-human CD11c clone EP1347Y	Abcam	ab52632	1 µl: 400 µl		<a href="https://www.abcam.com/cd11c-antibody-ep1347y-c-terminal-ab52632.html">https://www.abcam.com/cd11c-antibody-ep1347y-c-terminal-ab52632.html</a>
Anti-human CD206 clone 5C11	Abnova	H00004360-M02	1 µl: 1.500 µl		<a href="http://www.abnova.com/products/products_detail.asp?catalog_id=H00004360-M02">http://www.abnova.com/products/products_detail.asp?catalog_id=H00004360-M02</a>

#### DNA/cDNA Clones

Clone Name	Sequence	Source / Repository	Persistent ID / URL

#### Cultured Cells

Name	Vendor or Source	Sex (F, M, or unknown)	Persistent ID / URL

#### Data & Code Availability

Description	Source / Repository	Persistent ID / URL

#### Other

Description	Source / Repository	Persistent ID / URL

DOI [to be added]